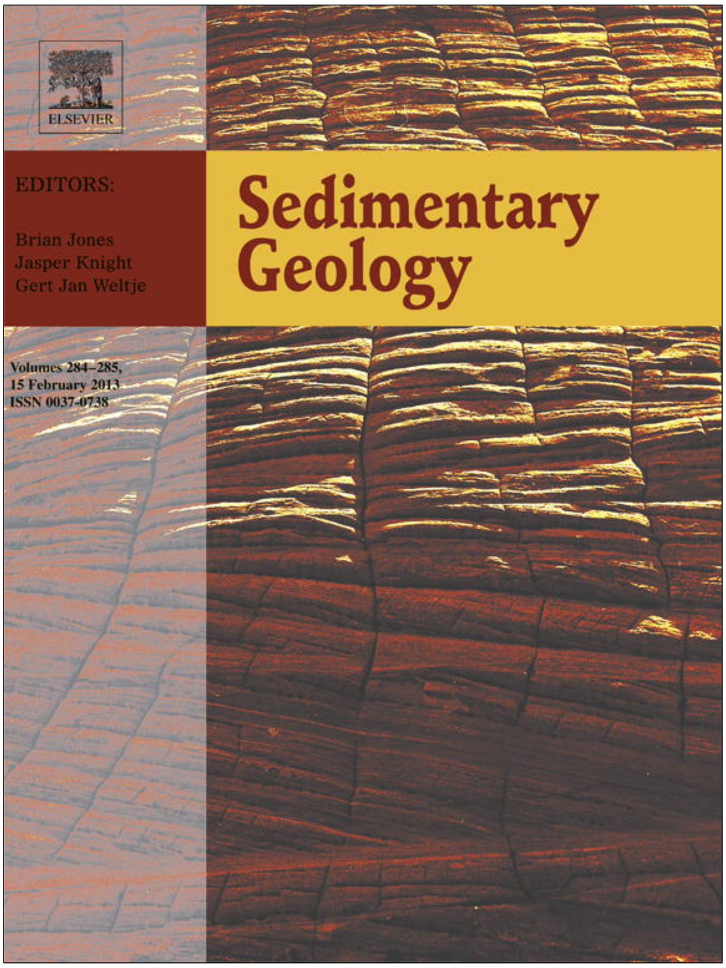
ELSEVIER
EDITORS:
Brian Jones
Jasper Knight
Gert Jan Weltje
Sedimentary Geology
Volumes 284–285,
15 February 2013
ISSN 0037-0738

Sedimentary Geology 284–285 (2013) 159–180

Contents lists available at SciVerse ScienceDirect

Sedimentary Geology

journal homepage: www.elsevier.com/locate/sedgeo

The transition from wave-dominated estuary to wave-dominated delta: The Late Quaternary stratigraphic architecture of Tiber River deltaic succession (Italy)

Salvatore Milli [a,*], Chiara D'Ambrogi [b], Piero Bellotti [a], Gilberto Calderoni [a], Maria Gabriella Carboni [a], Alessandra Celant [c], Letizia Di Bella [a], Federico Di Rita [c], Virgilio Frezza [a], Donatella Magri [c], Rita Maria Pichezzi [b], Valeria Ricci [b]

[a] *Dipartimento di Scienze della Terra, SAPIENZA Università di Roma, Piazzale A. Moro 5, 00185 Roma, Italy*
[b] *ISPRA, Servizio Geologico d'Italia, Via V. Brancati 48, 00144 Roma, Italy*
[c] *Dipartimento di Biologia Ambientale, SAPIENZA Università di Roma, Piazzale A. Moro 5, 00185 Roma, Italy*

ARTICLE INFO

Article history:
Received 3 April 2012
Received in revised form 22 November 2012
Accepted 7 December 2012
Available online 19 December 2012

Editor: G.J. Weltje

Keywords:
Late Quaternary sequence-stratigraphy
Climate change
Micropaleontology
Pollen
Plant macrofossils
Tiber delta

ABSTRACT

This paper presents a detailed description of the stratigraphic architecture of the Late Pleistocene/Holocene Tiber delta succession in order to document the passage from wave-dominated estuary to wave-dominated delta in the broader context of Late Quaternary sea level fluctuations.

This succession constitutes a sequence-stratigraphic unit known as Tiber Depositional Sequence (TDS), which was deposited during the last glacial–interglacial cycle (last 120 ka). Our study is based on the examination of an enormous amount of data derived from the stratigraphy of about 300 wells, petrographical and paleontological data (foraminifera, ostracoda, pollen, and plant macrofossils), ^{14}C dating, and from the integration of geomorphological and geoarcheological data. Recently a 100 m deep core (Pesce Luna well) was studied through a multidisciplinary approach and a detailed description of sedimentary facies, foraminifer and ostracod assemblages, pollen and ^{14}C dating is presented in this paper. The new data allowed to produce three new correlation panels and to describe in more detail, with respect to previous interpretations, the stratigraphic-depositional architecture of the TDS, which internally shows the preservation of sediment deposited during the early and late lowstand, the transgressive and the highstand systems tracts. Alluvial and coastal depositional systems characterize the early lowstand phase of the TDS, which developed during the eustatic sea-level fall between about 120 and 30–26 yr BP. During the late lowstand phase, which is characterized by stillstand and slow eustatic sea-level rise a prograding delta and an aggrading incised-valley fluvial fill developed. The Tiber incised valley was transformed into a wave-dominated estuary during the transgressive phase (TST), whereas a coastal-shelf sedimentation took place during the subsequent highstand phase (HST). This study confirms the lithofacies distribution resulting from transgression and infilling of the wave-dominated estuaries, but also shows how the transition to a wave-dominated delta, prograding at the time of sea-level highstand occurred. Changes in sediment input, climatic variations and, more recently, human activities played a major role in the development of the Tiber delta during the last 20,000 yr BP. In the last 3000 years a relationship between progradational phases of the delta and flood events of the Tiber river has been highlighted, suggesting also the formation and merging of barrier-spits to the mainland.

1. Introduction

In the recent decades, the late Quaternary deposits of the Mediterranean area have received much attention, thanks to the detailed investigations that have interested the deltaic and coastal plain successions, occurring mostly in subsurface and rarely in outcrop along the margins of this basin (see Coutellier and Stanley, 1987; Sestini, 1989; for the Nile delta; Oomkens, 1970; Boyer et al., 2005; Labaune et al., 2005 for the Rhône delta; Somoza et al., 1998; Hernández-Molina et al., 2000, for the Ebro delta; Ercilla et al., 1994; Hernández-Molina et al., 1996 for the Alboran Sea). In Italy many of these studies have focused on several aspects regarding depositional setting, climatic evolution and sequence-stratigraphic interpretation of the successions occurring along the coastal plain of the Tyrrhenian Sea (see Carboni et al., 2002; Bellotti et al., 2004; Aguzzi et al., 2007; Amorosi et al., 2011, for the Tuscany coastal plain; Bellotti et al., 1994, 1995; Amorosi and Milli, 2001; Giraudi et al., 2009, for the Tiber coastal plain; Barra et al., 1992; Ortolani and Pagliuca, 1999, for the Campania coastal plain) and of the Adriatic Sea, in particular the Po plain (see Amorosi and Milli, 2001; Amorosi et al., 2003, 2004; Amorosi and Colalongo, 2005). All these coastal plain and deltaic successions show strong similarities in terms

* Corresponding author. Tel.: +39 0649914157; fax: +39 064454729.
E-mail address: salvatore.milli@uniroma1.it (S. Milli).

0037-0738/$ – see front matter © 2013 Elsevier B.V. All rights reserved.
http://dx.doi.org/10.1016/j.sedgeo.2012.12.003

of stratigraphic architecture and evolution and this suggests, beyond local factors, that glacio-eustatic sea-level fluctuations related to Quaternary global climatic changes exerted a major control on sedimentation through the variation of accommodation space and base-level changes. Other factors, such as tectonics (uplift and subsidence), acted on a different scale, although their effects, taking into account the investigated time interval, can be considered negligible; in some cases it is possible, to evaluate the effects of local subsidence as an expression of sediment compaction and loading.

The main aim of this study is to document the change in depositional architecture of a Late Quaternary coastal system evolving from a wave-dominated estuary to a wave-dominated delta in response to relative sea-level fluctuations.

The Late Quaternary Tiber River deltaic succession (Tiber Depositional Sequence, TDS) records this change within its stratigraphic architecture, which has been reconstructed through the examination of a huge amount of data essentially derived from i) stratigraphy of about 300 wells, ii) petrographical, micropaleontological data (foraminifera, ostracoda and pollen analyses), iii) ^{14}C dating, and iv) integration of geomorphological and geoarcheological data (Belluomini et al., 1986; Bellotti et al., 1994, 1995, 2007, 2009, 2011; Chiocci and Milli, 1995; Giraudi et al., 2009; Di Rita et al., 2010; Di Bella et al., 2011). Recently a new borehole (Pesce Luna well, 100 m deep) was drilled during the survey of the sheet 386 Fiumicino of the Geological Map of Italy (1:50,000 scale). Samples of the sediment core allowed detailed biostratigraphical, sedimentological, pollen and plant macrofossil analyses, supported by ^{14}C dating.

The importance of this paper lies in the possibility of showing the sedimentary variability characterizing the Tiber deltaic succession, through integration of data sets that include the combined sedimentologic and micropaleontological (planktonic and benthic foraminifers, ostracods, pollen) study of several wells and cores. This data set also provides an example of evolution from continental to marine environments, which can be compared with other sedimentary successions developed, in the Mediterranean area, and in particular along margins of the Italian peninsula during the same interval of time.

Additional contributions of this paper are: 1) to highlight the stratigraphic relationships and stratal terminations observed through closely spaced well-log data sets, as well as to describe the physical characteristics of a high-frequency sequence, its systems tracts and associated surfaces; 2) to assess the mechanism of beach ridge accretion that developed during the highstand phase, which emphasizes the close interaction between flood events transporting large volume of sediment to subaqueous delta and the waves.

2. Geological and stratigraphic setting

The Tiber delta is located along the eastern margin of the Tyrrhenian Basin (Fig. 1), the youngest back-arc basin of the Mediterranean, developed since the Miocene as a consequence of rifting and back-arc extension related to the west-directed Apennines subduction (Scandone, 1980; Malinverno and Ryan, 1986; Savelli, 2002; Doglioni et al., 2004).

Along the Latium Tyrrhenian margin, the extensional tectonics characterizing this basin gave rise to the formation of half-graben basins, mainly oriented NNW–SSE/NW–SE, and subordinately NE–SW, which were filled with syn- and post-rift clastic sediments during the Pliocene and Pleistocene (Funiciello et al., 1976; Mariani and Prato, 1988; Barberi et al., 1994 and references therein) (Fig. 1b).

The Roman Basin, where the late Quaternary Tiber succession developed, is located in the central sector of Latium and extends north and south of Tiber River for about 135 km. The development of this basin started in the Late Pliocene and was accompanied by a continuous regional tectonic uplift (Milli, 1997; Bordoni and Valensise, 1998; Giordano et al., 2003), and by an intense volcanic activity, reaching a climax in the Middle-Upper Pleistocene, when the volcanic complexes of the Roman Magmatic Province developed (Locardi et al., 1976; Cioni et al., 1993; De Rita et al., 1993, 1995; Karner et al., 2001).

The stratigraphic framework of the Roman Basin is the result of the close interaction between tectonic uplift, volcanic activity and glacio-eustatic sea-level fluctuations which are also related to the Quaternary climatic changes (De Rita et al., 1994, 2002; Milli, 1994, 1997; Marra et al., 1998; Giordano et al., 2003; Milli et al., 2008). The stratal architecture of the basin is characterized by several depositional units constituting high-frequency depositional sequences with a duration variable from 30,000 yr to 120,000 yr (4th-order), stacked to form two composite 3rd-order sequences (*sensu* Mitchum and Van Wagoner, 1991), the Monte Mario Sequence (MMS; Lower Pleistocene) and the Ponte Galeria Sequence (PGS; Late Lower Pleistocene-Holocene), respectively (Milli, 1997; Milli and Palombo, 2011 with references therein) (Figs. 2 and 3). The MMS deposits crop out in the study area with a limited extension, and are essentially known through the stratigraphies of several wells. Such deposits are represented by coastal and transition-shelf depositional systems, developing during the Late Lowstand and Transgressive Systems tracts of MMS. The PGS strata are well-exposed. They contain fluvial, fluvio-lacustrine, barrier island-lagoon, and transition-shelf depositional systems, organised to constitute the lowstand (LST), the transgressive (TST), and the highstand (HST) systems tracts of the PGS (Fig. 3). Volcaniclastic deposits, belonging to the Albani and Sabatini volcanic complexes, are interfingered with these sediments and commonly constitute the filling of incised valleys.

In the studied area the PGS (from 10 to 110 m thick) lies above the shelfal mud sediments of the MMS through a polygenic erosional surface, formed during the sea-level fall characterizing the interval time between the MIS 31 and 27 (Fig. 2). This composite sequence consists of twelve 4th-order sequences (from 5 to 80 m thick) the boundaries of which are expressed by sharp erosional surfaces, recording basin- and downward shifts of facies, subaerial exposure and paleosoils in the interfluvial areas. The first and, four oldest 4th-order sequences (from PG01 to part of PG1) stack to form the late LST, which developed during a period of stillstand and slow relative sea-level rise producing a series of prograding and aggrading wedges-shaped high-frequency units. Sequences from PG1 to part of PG8 are referable to the TST, while the sequence PG9 (the Tiber Depositional Sequence, TDS) developed entirely during the HST (Fig. 2) (Milli and Palombo, 2011 Milli et al., in progress).

The stacking pattern of PGS shows a general trend characterized by a seaward stack of the fourth-order depositional sequences. This trend is opposite to the trend that PGS would display if controlled by glacio-eustasy alone. In this case, the equilibrium point of each fourth-order sequence should migrate progressively landward, confirming the trend visible on the eustatic curve (Haq et al., 1988; Hardenbol et al., 1998).

Consequently, the present setting of PGS is thought to be controlled by regional tectonic uplift, which forced the seaward migration of the fourth-order sequence equilibrium points, thus contributing to define the characteristic stacking pattern of PGS (see discussion in Milli, 1997).

3. Methods and data

The new correlation panels showing the depositional architecture of the PG9/TDS presented in this paper are the result of a close integration between literature data, the work developed in recent years consisting in the interpretation, from a depositional point of view, of the stratigraphic information from wells used in this work and the new data derived by the Pesce Luna well that will be described in detail in the following paragraphs. A grid of about 300 wells distributed on the Tiber delta plain, some of which with sediment cores, were used for this study (Fig. 4). Anyway, data from these wells (see Bellotti et al., 1994, 1995, 2007, 2009, 2011; Di Rita et al.,

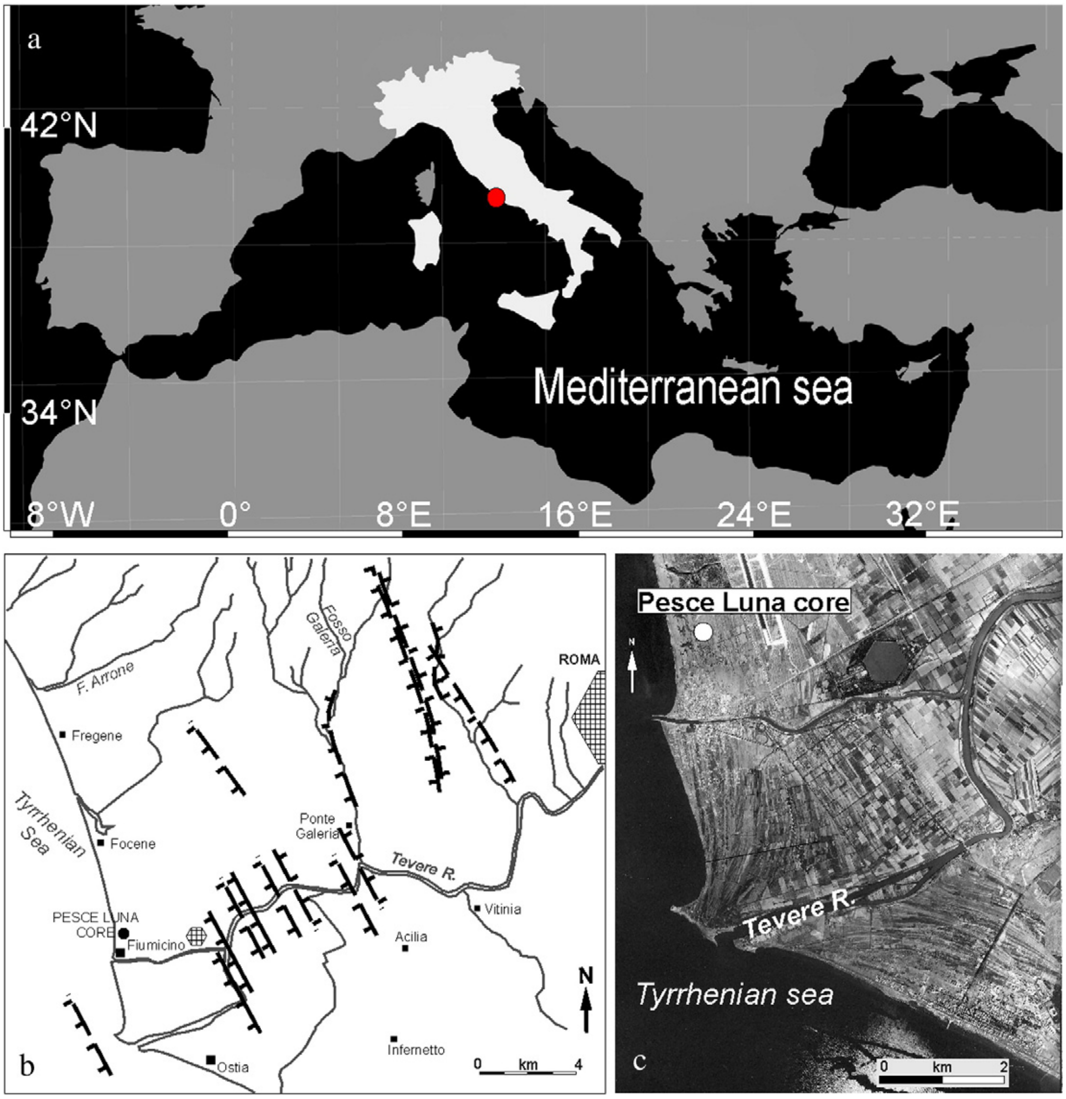

Fig. 1. a) Location of the studied area in the Mediterranean basin; b) main faults of the Roman basin, buried and inferred from seismic profiles; c) location of the Pesce Luna core.

2010; Di Bella et al., 2011) were reconsidered and reinterpreted in the light of the new results, and this allowed to better define the stratigraphic architecture of the Late Quaternary Tiber deltaic succession. Facies analysis derived by stratigraphic interpretation of the several wells together with microfaunistic and pollen analyses from literature data (see previous references), and Pesce Luna well turned out to be fundamental in order to discriminate the different sedimentary environments and to investigate the recurring cyclic pattern (scale of parasequences) recognised in the succession. Calibrated radiocarbon dating allowed framing the resulting stratigraphic-depositional stacking pattern into a sequence-stratigraphic context.

4. The Pesce Luna core

The Pesce Luna well (100 m-long) was drilled close to the Fiumicino village, 5 km north of the main Tiber River mouth (Fig. 1). The drilling method consisted of a double corer, having a diameter of 12 cm; the recovery of the core was more than 95%. The description of the core was made after it was split into two parts for its entire length. Grain size and other textural attributes, as well as sedimentary structures and color were the main described features. Other aspects such as the presence of shelly debris, clasts of clay, organic matter, wood fragments, peat and roots were also taken into consideration as useful features for environmental interpretation.

The Pesce Luna well crosses a succession (from top to bottom) including: 1) the deposits of Tiber Depositional Sequence, 2) a thick (6 m) sandy gravel body that basing on the stratigraphy of the outcropping deposits, is fluvial in origin and belongs to one of the lowest fourth-order sequences (Sicilian, Lower Pleistocene) forming the lowstand system tracts of the PGS, and 3) the Lower Pleistocene (Santernian–Emilian) silty clay and clay deposits ascribed to the MMS (Fig. 5). These three recognised units are separated by erosive surfaces (unconformities) marking significant hiatuses; they are evidenced by important changes of facies.

In this work we describe in detail the upper 50 m portion of the Pesce Luna core, corresponding to the TDS. This part of the borehole shows great variability of the depositional environments passing, from bottom to top, from lagoon to shelf, and from shoreface to beachface, recording the transition from transgressive to highstand systems tracts of the TDS in the last 15,000 years. This trend is also suggested by micropaleontological data. Methods utilized for the micropaleontological and radiocarbon analyses are reported in the supplementary online material (SOM).

4.1. Foraminiferal and ostracod analysis

Results of quantitative analysis and diversity indices (see SOM) allowed to recognizing three different foraminiferal assemblages (Table 1).

F1 assemblage is characterized by low species diversity (mean α-index 3.94; mean Shannon-index 1.46) and the dominance of *Ammonia parkinsoniana*; accompanying taxa are *Ammonia tepida* and *Haynesina germanica*.

F2 assemblage includes samples characterized by the dominance of *A. parkinsoniana*; accompanying taxa are *A. tepida* and *Aubygnina perlucida*. This assemblage records specific diversity with mean values of 5.69 and 1.94 for α-index and H, respectively. Other species like

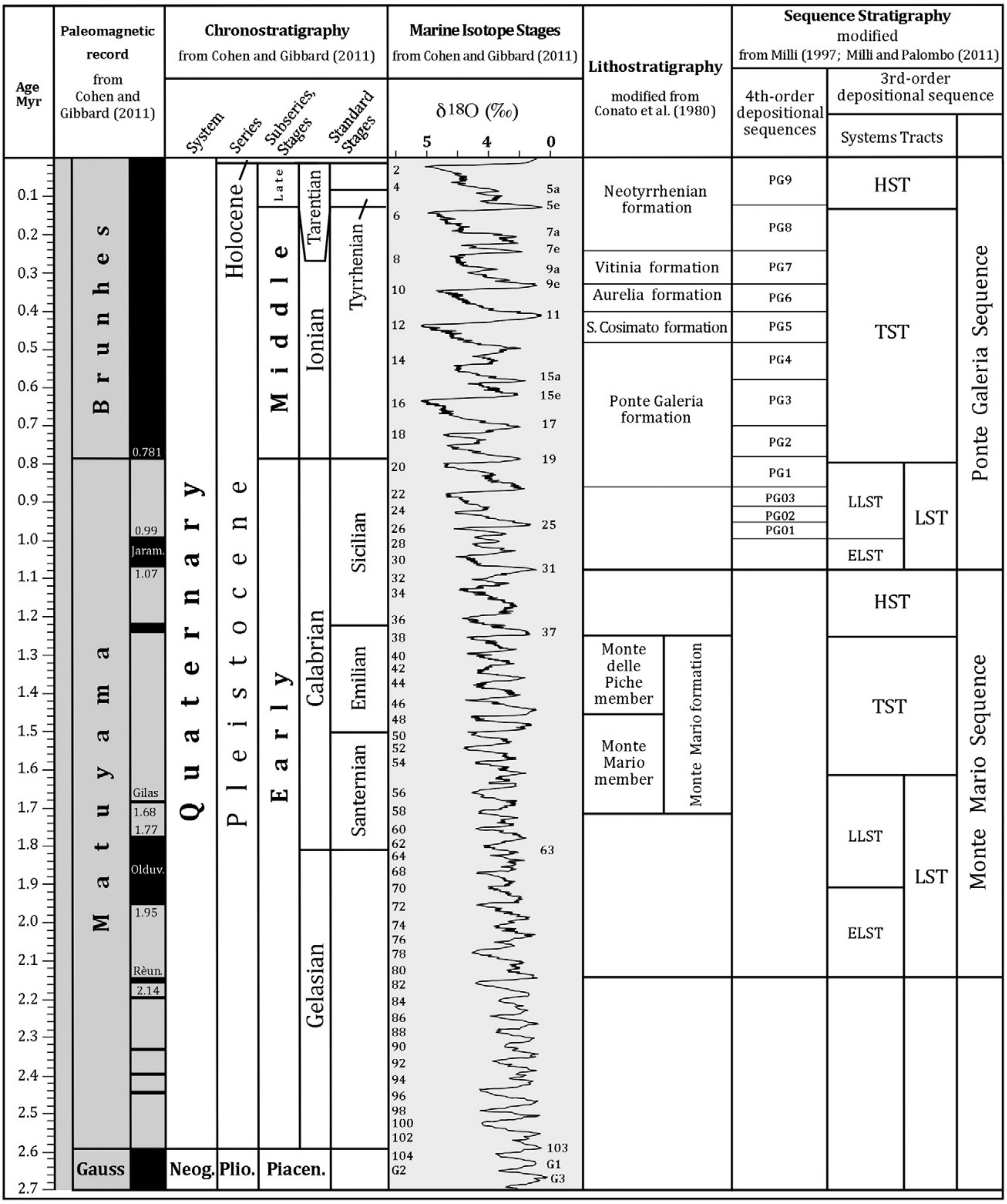

Fig. 2. Chronostratigraphic and sequence-stratigraphic scheme of the Pleistocene deposits of the Roman Basin (after Milli, 1997; Milli and Palombo, 2011). HST: Highstand Systems Tract; TST: Transgressive Systems Tract; LST: Lowstand Systems Tract; ELST: Early Lowstand Systems Tract; LLST: Late Lowstand Systems Tract.

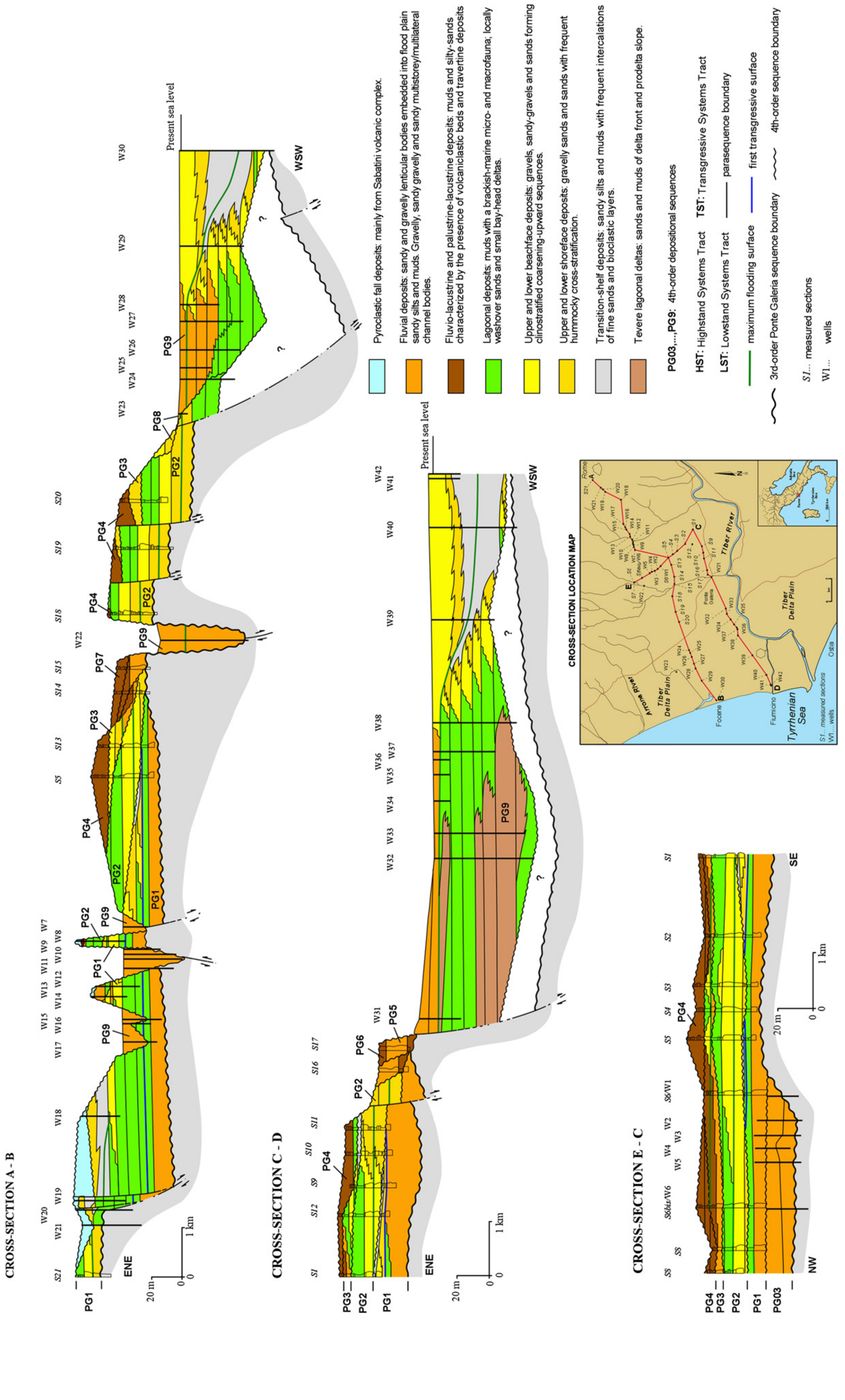

Fig. 3. Stratigraphic cross-section of the Ponte Galeria Sequence (PGS). Modified after Milli (1997).

Elphidium poeyanum, *Ammonia beccarii*, *Elphidium advenum*, and miliolids generally common in normal marine infralittoral environment, are found.

F3 assemblage shows the dominance of *Ammonia* spp. Accompanying taxa are *E. poeyanum* and miliolids. This assemblage is characterized by a higher diversity degree (mean α-index 11.37; mean Shannon-index 1.67) and the increase of shallow marine species (*A. beccarii*, *E. poeyanum*, *Elphidium. granosum*, *E. advenum*, *Quinqueloculina* spp. and *Triloculina* spp.).

Plankton is scarce in all three assemblages. Anyway, the highest frequencies (10.95%) are recorded in F3 assemblage while the lowest values (<3%) are found in F1 and F2 assemblages. The most frequent species are *Globigerina bulloides*, *Globigerinita glutinata*, *Globigerinoides ruber* and *Turborotalita quinqueloba*.

Regarding ostracods the recognized assemblages suggest, coherently with the foraminifera data, a passage from brackish lagoon oligotypic fauna to open lagoon/marine fauna, from the bottom to the top of the core (Table 1).

4.2. Pollen and plant macrofossil analysis

Pollen and plant macrofossil analyses allowed to recognize within the Pesce Luna well, from the base upward, five pollen zones (from PLU 1 to PLU 5; Fig. 6), and four plant macroremain zones (from PLU A to PLU D; Fig. 7), respectively.

The pollen record reflects both vegetation changes determined by the global climate fluctuations of the late glacial and beginning of the Holocene, as discussed below, and local environmental shifts, related to hydrological changes. The plant macrofossil record shows the local aquatic conditions of the basin.

4.3. Radiocarbon dates

Radiocarbon datings were derived by the analysis of 8 samples obtained from wood, peat and organic-rich layers collected at various depths between 10 and 45 m (Table 2).

The eight ^{14}C readings range from 1390–1290 (viz, 560–660 AD) to 15,250–14,150 cal BP. They are of some concern in that allows us to asses a detailed chronostratigraphy of the drilled sediments since the late Pleniglacial up to the early Holocene. Due to the complex sediment array, a direct correlation between age and depth in core is lacking. However, with the obvious exception of sample Rome-2137 (dated at historical times), it is observed that all the samples older than 12,000 yr BP are from depths in core from ca. −37 to ca. −44 m.

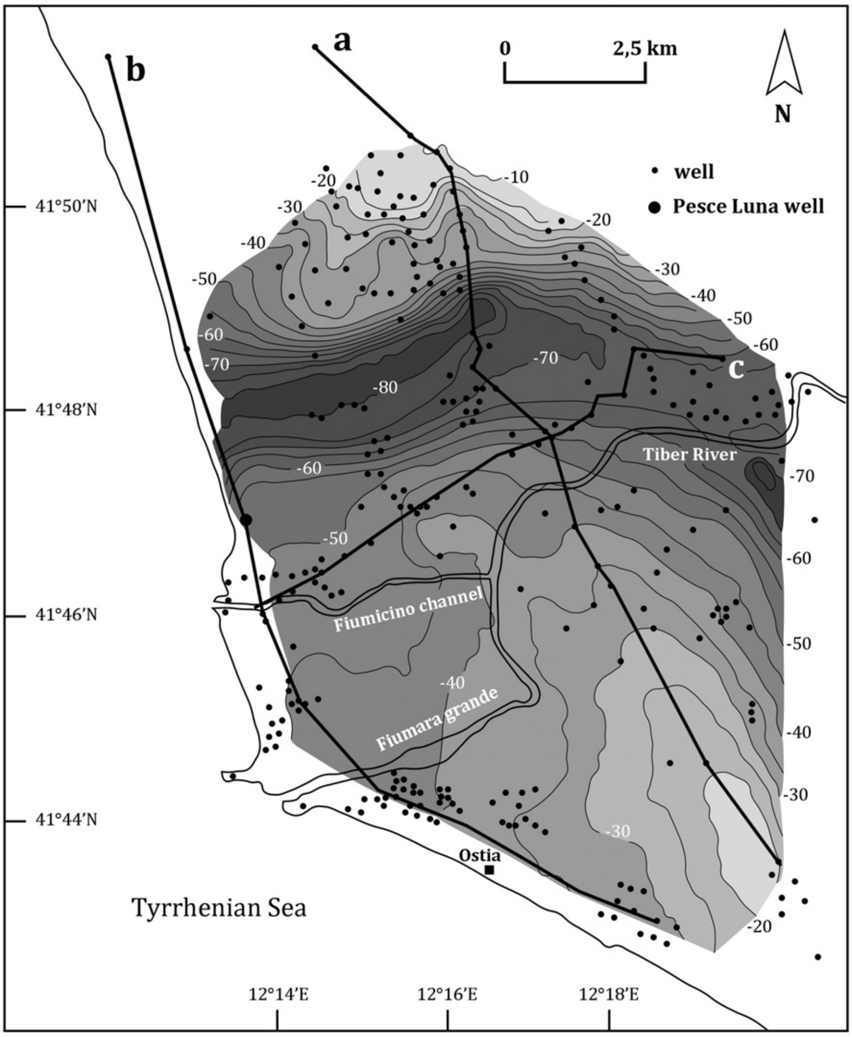

Fig. 4. Structure contour map of the unconformity at the base of the Tiber Depositional Sequence (in metres with respect to present sea-level. Map shows also the location of the wells utilized in the present study and the tracts of the cross-sections of Fig. 9.

In order to better constrain the age of deposits and of the main stratigraphic surfaces we have also utilized the ^{14}C data sets from the literature (Belluomini et al., 1986; Bellotti et al., 2007, 2011; Di Bella et al., 2011). A complete list of radiocarbon datings on Tiber delta deposits, consisting of 62 calibrated dates, is reported in the supplementary online material.

4.4. Description and paleoenvironmental interpretation of Pesce Luna core

Based on data obtained from the analysis described above the investigated portion of Pesce Luna well can be divided into a series of depositional units corresponding to different depositional environments and subenvironments, each characterized by a different facies association. The sedimentological and micropaleontological (ostracods, foraminifers, and pollen) characteristics of these units will be described in ascending order.

4.4.1. Estuary

The facies associations related to this environment show a considerable variability and can be subdivided into three main facies associations (A, B, C) (Figs. 5 and 6; Table 1).

Facies association A (Fig. 6a, a′) developed between −48.60 and −42 m. It is composed by clay and locally peaty clay with widespread organic matter. Shell debris are absent below −48 m, are rare in the lower part, and are found in the upper part of this interval. Between −48.60 and −48 m the sediment is composed of clay containing thin levels of coarse sand and gravel; it represents a transgressive lag directly placed on the TDS sequence boundary separating this unit from the underlying fluvial and coastal Middle Pleistocene gravel, belonging to one of the high-frequency depositional sequences of the third-order Ponte Galeria Sequence.

Foraminifera and ostracods are absent throughout this interval. The pollen assemblage between −44.50 and −43.45 m (Zone Plu-1) suggests an open landscape dominated by xerophytes and grasses with non-arboreal pollen (NAP) percentages between 40% and 90%. High percentages of herbs and low palynological richness (13 taxa) at the base of the record are likely to result from selective preservation of pollen grains of local origin, mainly represented by oxidation-resistant pollen of xerophytic herbs and other NAP, like Cichorioideae and Chenopodiaceae (Bottema, 1975; Havinga, 1984). Over representation of pollen of local origin may have partly affected the percentage representation of the arboreal vegetation in the lower part of zone. Towards the end of the zone, a remarkable increase in trees is recorded: deciduous trees (30%) and *Pinus* (20%) are the main elements of the woody vegetation, although a general increase in all the arboreal components is recorded. Below this zone the pollen record is interrupted for the scarcity of pollen in the sediment samples. Plant macroremains have been recognized between −43.50 and −40 m (Zone Plu-A); the most abundant taxon is *Juncus* spp., continuously represented, accompanied by discontinuous appearances of *Carex elata* and two species of *Typha*. On the whole, they outline a marshy landscape with local ponds. Halophilous taxa are absent in this freshwater environment.

Facies association B (Fig. 6b) characterizes the interval between −42 and −36.80 m, and consists of grey silty clay and clay with widespread organic matter (essentially plant debris), peaty layers between −37.70 and −37.40 m and between −38.80 and −38.60 m, and thin shell debris layers. Millimetric sandy levels occur between −41 and −40 m.

The foraminiferal assemblage (F1) records a sharp reduction in specific diversity, which gives to it an oligospecific character. Dominant species is *A. parkinsoniana*, at which are associated other species as *A. perlucida*, *Haynesina depressula*, *H. germanica* and *E. granosum*. Such assemblage suggests a typical brackish, lagoon–marsh environment (Fiorini and Vaiani, 2001; Carboni et al., 2002; Bergamin et al., 2006) or brackish-water lagoon (Amorosi et al., 2004).

Ostracods related to facies association B are more differentiated with respect to the foraminiferal assemblage. The interval between −37.4 and −36.6 m is dominated by *Cyprideis torosa*, but is characterized by relatively high diversity. Other brackish-water species as *Loxoconcha elliptica* and *Loxoconcha stellifera* (Pugliese and Stanley, 1991; Carboni et al., 2002) are present. Moreover, the marine species *Propontocypris pirifera* is found in the interval −37.2/−36.9 m. Nevertheless this taxon may also be present in brackish environments (Mazzini et al., 1999; Guernet et al., 2003). The interval −38.3/−37.5 m is barren, whereas between −39 and −38.4 m (with −38.7 m barren), there is a transition from oligotypic to monospecific assemblages dominated by *C. torosa*. Monospecific assemblages of *C. torosa* are interpreted to represent environmental stress. This species typical of brackish-water and lagoonal environments is also highly euryhaline, showing an adaptability to salinities from 0.4 to 150‰ (Neale, 1988) and therefore an opportunistic behavior (Frenzel and Boomer, 2005). According Ruiz Muñoz et al. (2006, and references therein) in the natural filling of coastal lagoons, the diminution of the hydrodynamic gradient and the presence of higher salinities cause the progressive replacement of *L. elliptica* by *C. torosa*, which become almost monospecific. The interval −40.6/−39.5 m is again barren, whereas between −39.5 and −39.1 m an assemblage with *Aurila woodwardi*, *Leptocythere lagunae*, *L. elliptica* and *Palmoconcha turbida* was found. *A. woodwardi*, *L. lagunae* and *L. elliptica* are brackish-water or lagoonal taxa (Pugliese and Stanley, 1991; Montenegro and Pugliese, 1995, 1996), whereas *Palmoconcha turbida* is considered as an opportunistic species whose tolerance to low oxygen permits its survival in hypoxic environments (Bodergat et al., 1998; Ruiz Muñoz et al., 2005). In the interval −42.2/−40.6 m, an oligotypic assemblage was found. It is characterized by the presence of typical brackish-water or lagoonal species as *C. torosa* and *L. elliptica* diffused in recent Mediterranean lagoons (Pugliese and Stanley, 1991; Montenegro and Pugliese, 1995, 1996; Carboni et al., 2002; Cabral et al., 2006). *C. torosa* and *L. elliptica* are clearly associated with all the different transitional environments between fresh and marine waters with strong trophic gradients and high salinity variability (Carbonel, 1982). In the lowermost portion of this interval, barren levels and levels containing only juvenile valves of *C. torosa* were found. Moreover, the presence of *Potamocypris* sp., testifies a fresh-water contribution (Carboni et al., 2002).

Pollen data from this facies association indicate the presence of a well-developed marshland, mainly composed of sedges and rushes (Cyperaceae and Juncaceae) between −42.05 and −40.65 m pollen (Zone Plu-2). The coeval record of aquatic plants and the remarkable amount of fragments of cyanobacteria of the Rivulariaceae family, often involved in eutrophication processes (Aavad, 1994), suggest enrichment of nutrients in the basin. The landscape experienced an important increase in the arboreal vegetation (AP + *Pinus* 79%). The woodland was dominated by deciduous trees (>50%) with stands of thermophilous communities with evergreen elements (10%). The increase in (25%) may be partly related to long-distance transportation. The interval between −40.65 and −39.15 m (Zone Plu-3), records an important decrease in broadleaved vegetation, determined by an abrupt drop of deciduous trees (down to 11%) and a steady decline of evergreen elements. Nevertheless, tree percentages keep high values due to a further increase in *Pinus* (40%). The pollen record outlines a deforested landscape with the development of open vegetation dominated by xerophytes (20%) and local sedges/rushes communities (20%). In the interval between −39.15 and −37.40 m (Zone Plu-4) a new development of all the broadleaved trees, paralleled a drop of *Pinus*. Peaks of grasses (>45%), sedges/rushes (43%), aquatics (15%), riparian trees (15%) and Rivulariaceae (22%) suggest the presence of a wide and unstable marshland, with euthrophic ponds. These local vegetation elements are likely to affect the percentage representation of the regional arboreal vegetation, showing an abrupt decrease (35%) while pollen concentrations show high values.

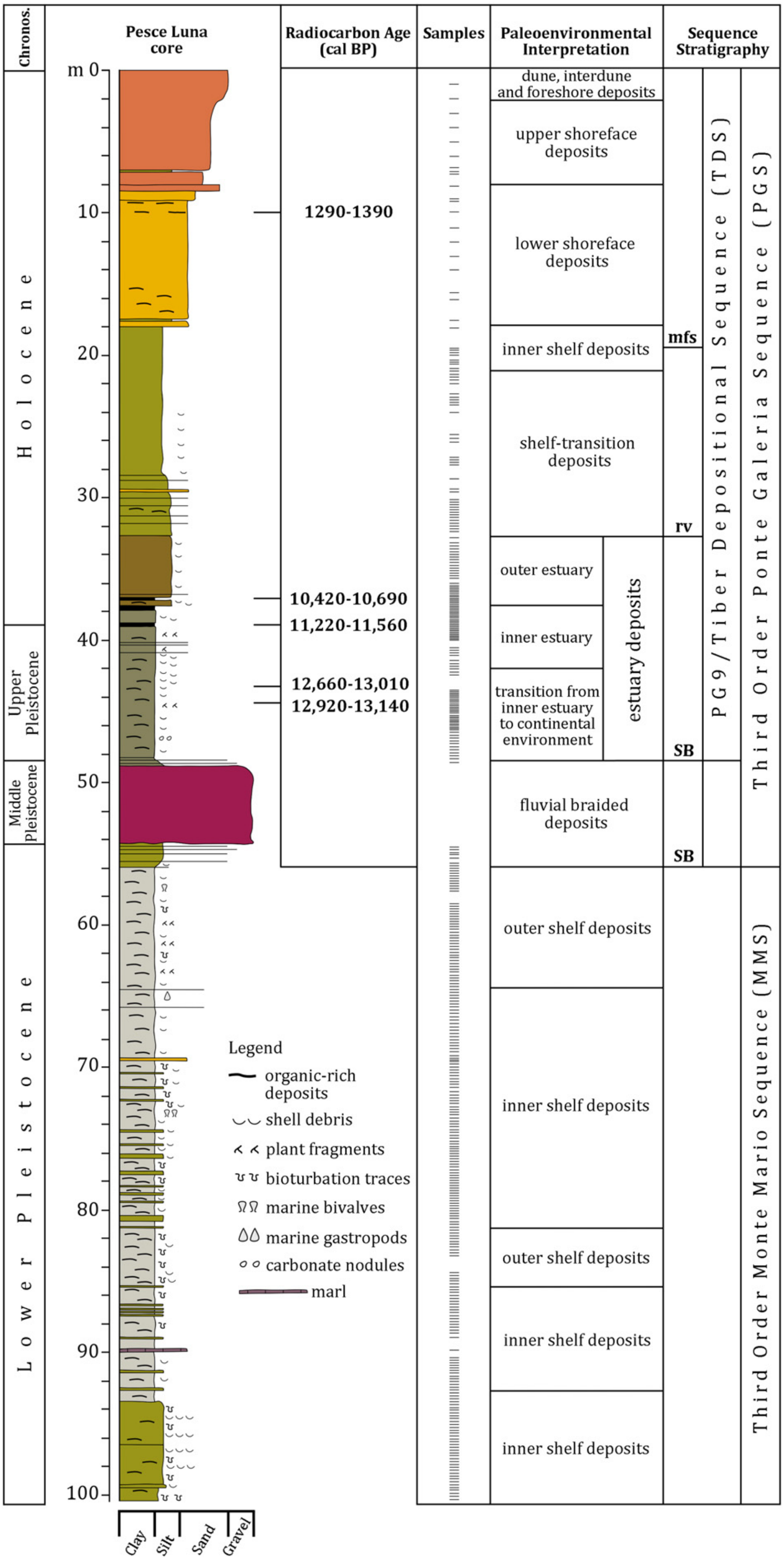
Chronos.
Pesce Luna core
Radiocarbon Age (cal BP)
Samples
Paleoenvironmental Interpretation
Sequence Stratigraphy
m 0
10
20
30
40
50
60
70
80
90
100
Holocene
Upper Pleistocene
Middle Pleistocene
Lower Pleistocene
1290-1390
10,420-10,690
11,220-11,560
12,660-13,010
12,920-13,140
dune, interdune and foreshore deposits
upper shoreface deposits
lower shoreface deposits
inner shelf deposits
shelf-transition deposits
outer estuary
inner estuary
transition from inner estuary to continental environment
estuary deposits
fluvial braided deposits
outer shelf deposits
inner shelf deposits
outer shelf deposits
inner shelf deposits
inner shelf deposits
mfs
rv
SB
SB
PG9/Tiber Depositional Sequence (TDS)
Third Order Ponte Galeria Sequence (PGS)
Third Order Monte Mario Sequence (MMS)
Legend
organic-rich deposits
shell debris
plant fragments
bioturbation traces
marine bivalves
marine gastropods
carbonate nodules
marl
Clay
Silt
Sand
Gravel

Table 1
Foraminiferal and ostracod assemblages of Pesce Luna core.

Facies		Estuary Facies association A	Estuary Facies association B	Estuary Facies association C	Upper and lower shoreface Inner shelf Shelf-transition
Foraminifera	Assemblages	No forams	F1	F2	F3
	Alpha-index		3.94	5.69	11.37
	Shannon-index		1.46	1.94	1.67
	Dominant taxa		*A. parkinsoniana*	*Elphidium granosum* *Ammonia parkinsoniana*	*Ammonia* spp.
	Accompanying taxa		*Ammonia tepida* *Haynesina germanica*	*Ammonia tepida* *Aubygnina perlucida*	*Elphidium poeyanum* miliolids
Ostracods	Dominant taxa	No ostracods	*Cyprideis torosa*	*Carinocythereis antiquata* *Cytherois fisheri* *Leptocythere bacescoi* *Leptocythere lagunae* *Leptocythere ramosa* *Loxoconcha subrugosa* *Propontocypris pirifera* *Semicytherura incongruens*	*Palmoconcha turbida* *Pontocythere turbida*
	Accompanying taxa		*Aurila woodwardi* *Leptocythere lagunae* *Loxoconcha elliptica* *Loxoconcha stellifera* *Propontocypris pirifera*		*Carinocythereis antiquata* *Leptocythere ramosa* *Semicytherura incongruens*

Plant macroremains show, that various species of *Juncus* dominated a marshy environment in the interval between −40 and −39 m (Zone Plu-B). The presence of *Cyperus fuscus* and of *Chenopodium* sp. suggests a lowering of the water level compared to the overlying zone and exposure of sandy soils. In the interval between −39/−37 m (Zone Plu-C), a clear environmental change is marked by the introduction of new taxa, namely *Cladium mariscus*, *Ruppia maritima*, *Carex riparia*, and *Rumex* sp., accompanying the taxa already present in the overlying zone (*Juncus* spp., *Typha latifolia*, *T. angustifolia* and *C. elata*). A mosaic of marshes (*Typha* and *C. riparia*) and wet meadows (*C. mariscus*) with nitrophilous elements (*Rumex* sp.) developed. Brackish conditions are suggested at the base of the interval by *R. maritima*.

Facies association C (Fig. 6c) developed between −36.80 and −33 m and is composed of grey clay with a few silt intercalations and a thin sand layer in the lowermost portion (−36.70 m). Wood fragments and shell debris are scattered throughout this interval.

The foraminiferal assemblage (F2) records a higher specific diversity with respect to F1 assemblage and is characterized by typical taxa of shallow water environments with significant organic matter content (*E. granosum* and *A. parkinsoniana*, Jorissen, 1988) and taxa of normal marine infralittoral environment (*E. poeyanum*, *A. beccarii*, *E. advenum* and miliolids). Moreover the presence of high percentage of *A. tepida* and *Nonionella turgida* may suggest, nutrient-rich conditions characterized by wide availability of food, with no oxygen depletion (Jorissen, 1988; Van der Zwaan and Jorissen, 1991; Barmawidjaja et al., 1992).

Ostracods assemblages show some variability. From −36.5 to −35.55 m, *C. torosa* disappears and the ostracod assemblage becomes more diversified. The principal taxa are *Leptocythere bacescoi*, *L. lagunae* and *P. pirifera*, which can be considered as brackish-water/marine forms (Mazzini et al., 1999). An assemblage of brackish-water/marine species characterizes the interval −35.4/−34 m. *Cytherois fisheri* (Carboni et al., 2002), *Carinocythereis antiquata*, *Loxoconcha subrugosa* and *Semicytherura incongruens* are abundant in this interval and are indicative of estuarine environment (Pugliese and Stanley, 1991; Montenegro et al., 1998). Ostracod assemblages are characterized by a dominance of marine littoral species as *Leptocythere ramosa* and *L. subrugosa* (Montenegro et al., 1998) in the interval from −33.8 to −32.2 m.

Pollen analysis indicates for this interval (Zone Plu-5) a strong reduction of grasses, sedges/rushes and aquatic plant, so that herb percentages decreased to 15%, although significant amounts of xerophytes and other herbs are still recorded. This would suggest a strong reduction of marshy environments. The landscape was dominated by deciduous trees, which were the main component of the planitial forest; a clear increase in evergreen elements is recorded, indicating the development of a *macchia*, a typical community of the local coastal environment. Plant macroremains (Zone Plu-D), indicate an increase in salinity as evidenced by a significant abundance of *Chenopodium* sp. The disappearance of *C. mariscus*, *Juncus* spp. and *Carex* spp. suggests a marked reduction of the wetland in favour of sandy soils populated by *Cyperus flavescens* and *C. fuscus* (Figs. 7 and 8).

The integration among sedimentological, microfaunistic, pollen and plant macrofossil data suggests that the deposition of the three facies associations took place within a wave-dominated estuary (*sensu* Dalrymple et al., 1992; Boyd et al., 2006) and in particular in the central portion of the estuary where the low-energy part occurs. The three facies associations can be attributed to three distinct environments. The *facies association C*, having brackish-water/marine species microfaunistic assemblages and a pollen and vegetational assemblages typical of a coastal environment with increase of salinity, suggests deposition in an outer estuary environment. Here the possibility of exchange between marine and lagoonal environments is strongly favoured through the inlets cutting the seaward coastal barrier. The *facies association B* is characterized by microfaunistic and pollen assemblages and plant macroremains suggesting a brackish, lagoon–marsh environment with eutrophic ponds subject to water level changes; this allowed to interpret this facies association as the product of the sedimentation in the inner estuary. The *facies association A* is also attributed to this sector as it is characterized by the absence of microfauna, a feature that for the ostracods can be related to a continental sedimentation probably linked to fluvial processes (Cabral et al., 2006), and by pollen and plant macrofossil assemblages indicating an open landscape with a strong fluvial influence.

Fig. 5. Stratigraphic column of Pesce Luna core showing the inferred depositional environment and the sequence stratigraphic interpretation. SB: sequence boundary; rv: ravinement surface; mfs: maximum flooding surface.

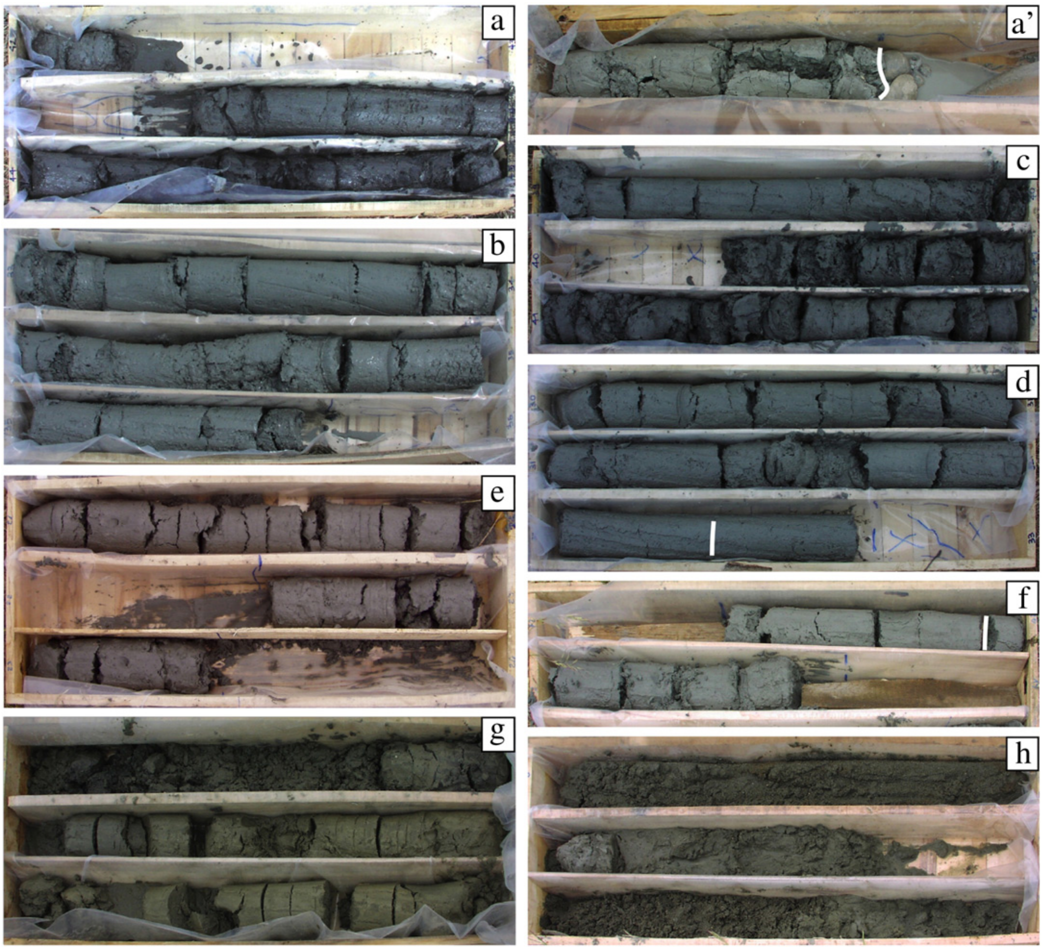

Fig. 6. Representative photographs of Pesce Luna core. Estuary deposits: a′) core depth −48 −49 m, a) core depth −42 −45 m, (facies association A); red line indicates the sequence boundary of TDS; b) core depth −39 −42 m (facies association B); c) core depth −33 −36 m (facies association C). Shelf-transition deposits: d) core depth −30 −33 m (light blue indicates the ravinement surface; for its position see Fig. 9b); e) core depth – 21 −24 m. Inner shelf deposits: f) core depth −18 −21 m (green line indicates the maximum flooding surface; for its position see Fig. 9b). Lower and upper shoreface deposits: g) core depth −9 −12 m; h) core depth −6 −9 m.

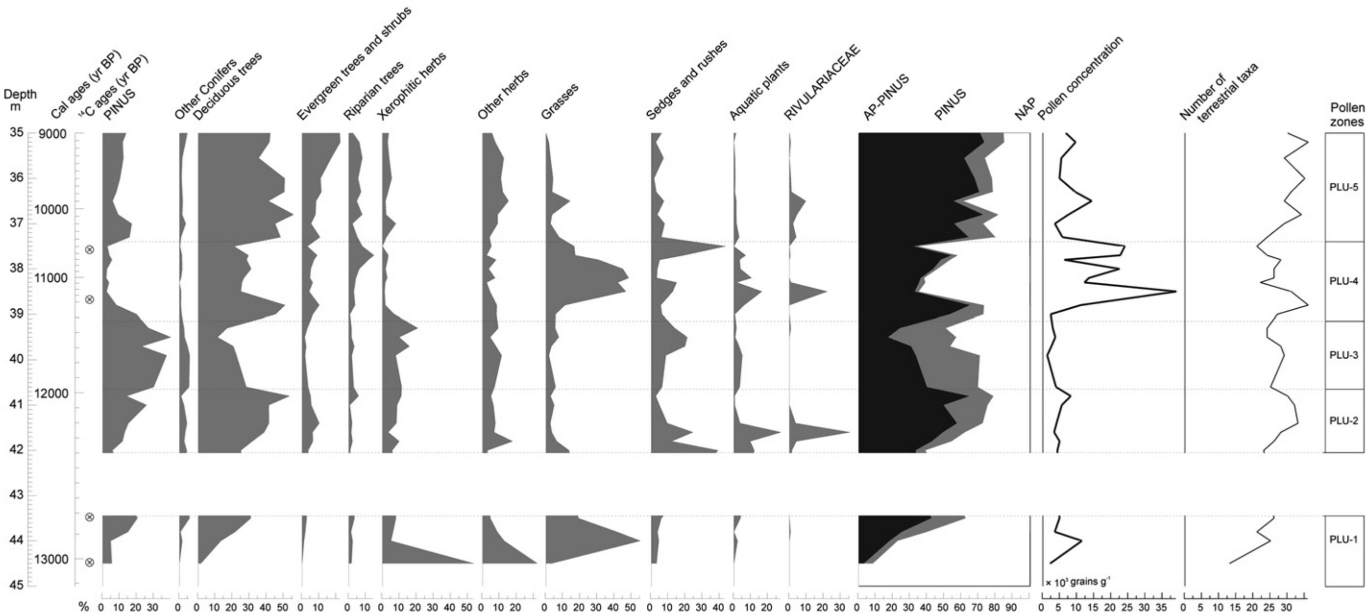

Fig. 7. Pollen percentage diagram from the Pesce Luna core.

Table 2
^{14}C readings yielded by the organic matter in the Pesce Luna core samples.

Sample identifier	Samples	Core-depth in m	Material	Conventional ^{14}C age (yr BP)	Calibrated age $^{(1)}$ (cal BP)	δ ^{13}C $^{(2)}$ (‰, vs. PDB)
Rome-2137	PL13	−10.0	Organic sand	1445±50	1390–1290	−27.0
Rome-2138	PL87	−36.9	Peaty clay	10,390±80	12,650–11,950	−24.9
Rome-2143	PL94	−37.6	Peat	9345±75	10,690–10,420	−23.6
Rome-2142	PL105	−38.7	Peat	9955±80	11,560–11,220	−24.7
Rome-2141	PL120	−40.8	Organic clay	12,445±90	15,250–14,150	−25.8
Rome-2144	PL128	−43.5	Organic clay	10,835±85	13,010–12,660	−23.3
Rome-2139	PL138	−44.4	Peaty clay	10,960±80	13,140–12,900	−23.7
Rome-2140	PL136/138	−44.3/−44.5	Peaty clay	11,010±85	13,150–12,940	−258
Weighted means for Rome-2139 and -2140				10,985±60	13,140–12,920	−24.9

(1) Calibration performed with the software after Ramsey (2005).
(2) Uncertainty ranges from ±0.25 to ±0.15‰.

The superimposition of the three facies association, from lowermost to uppermost part of the core evidences a clear transgressive trend, which is confirmed by the overlying transition-shelf and inner shelf deposits.

4.4.2. Shelf-transition

The deposits related to this environment have been subdivided into two facies associations (Figs. 5 and 6; Table 1). The first facies association (Fig. 6d), between −33 and −28.5 m, is constituted by an alternation of silty clay and very fine sandy levels with frequent plant and shell debris. The foraminiferal assemblage is F3; dominant species are *A. parkinsoniana* and *E. poeyanum*, although it is observed a substantial increase of *A. beccarii* a species that is abundant in infralittoral sandy bottoms (Sgarrella and Moncharmont-Zei, 1993; Bellotti et al., 1994; Ruiz Muñoz et al., 1996; Mendes et al., 2004; Frezza and Carboni, 2009). An increase of miliolids and in particular of *Triloculina* spp. and *Adelosina* spp is also observed. In the ostracoda assemblage the dominant species are *Palmoconcha turbida* and *Pontocythere turbida*. No pollen has been found in these deposits. The absence or the sharp decrease of fauna recorded in some samples as well as the local increase of plankton is thought to be due to the great variability of the ecological and physical factors that characterize infralittoral environments. No pollen is found in this facies association.

The second facies association (Fig. 6e), developed between −28.5 and −21 m, is constituted by silty clay deposits with scattered shell debris, which decrease from bottom to top of the interval. The

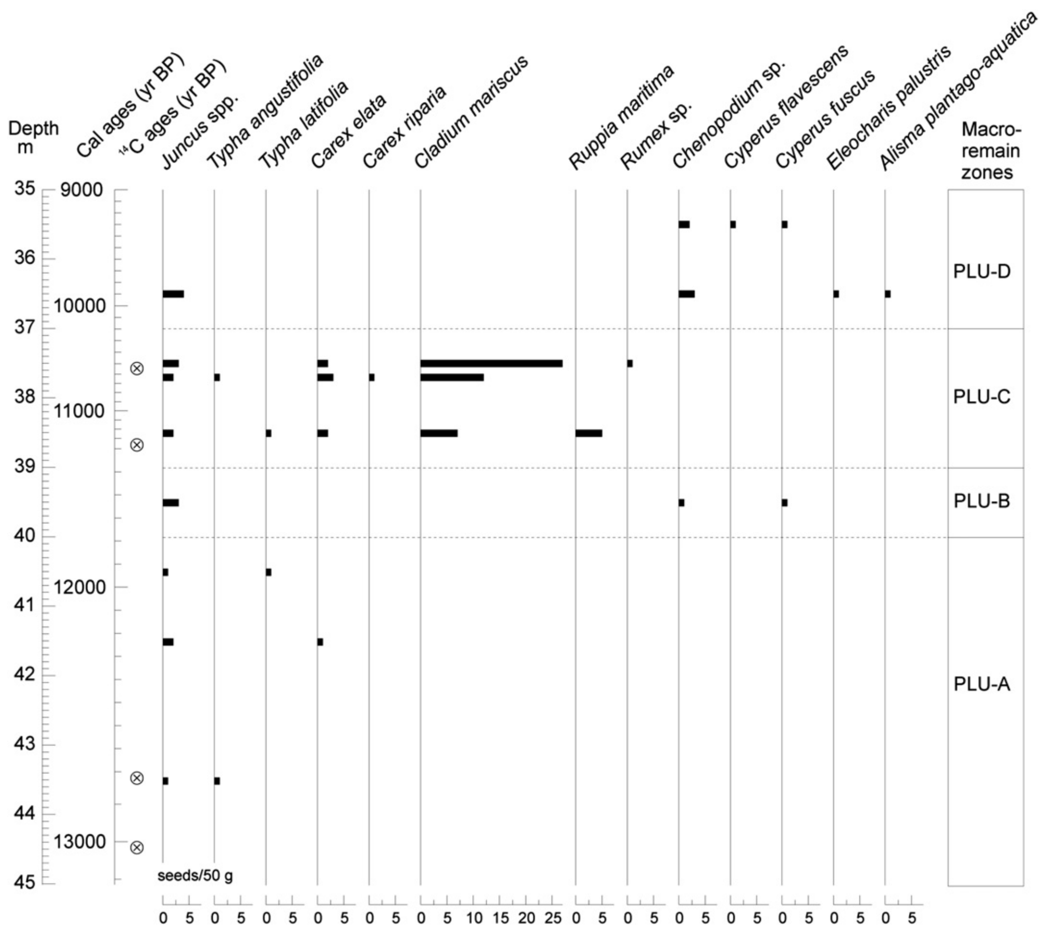

Fig. 8. Plant macroremains concentration diagram of Pesce Luna core.

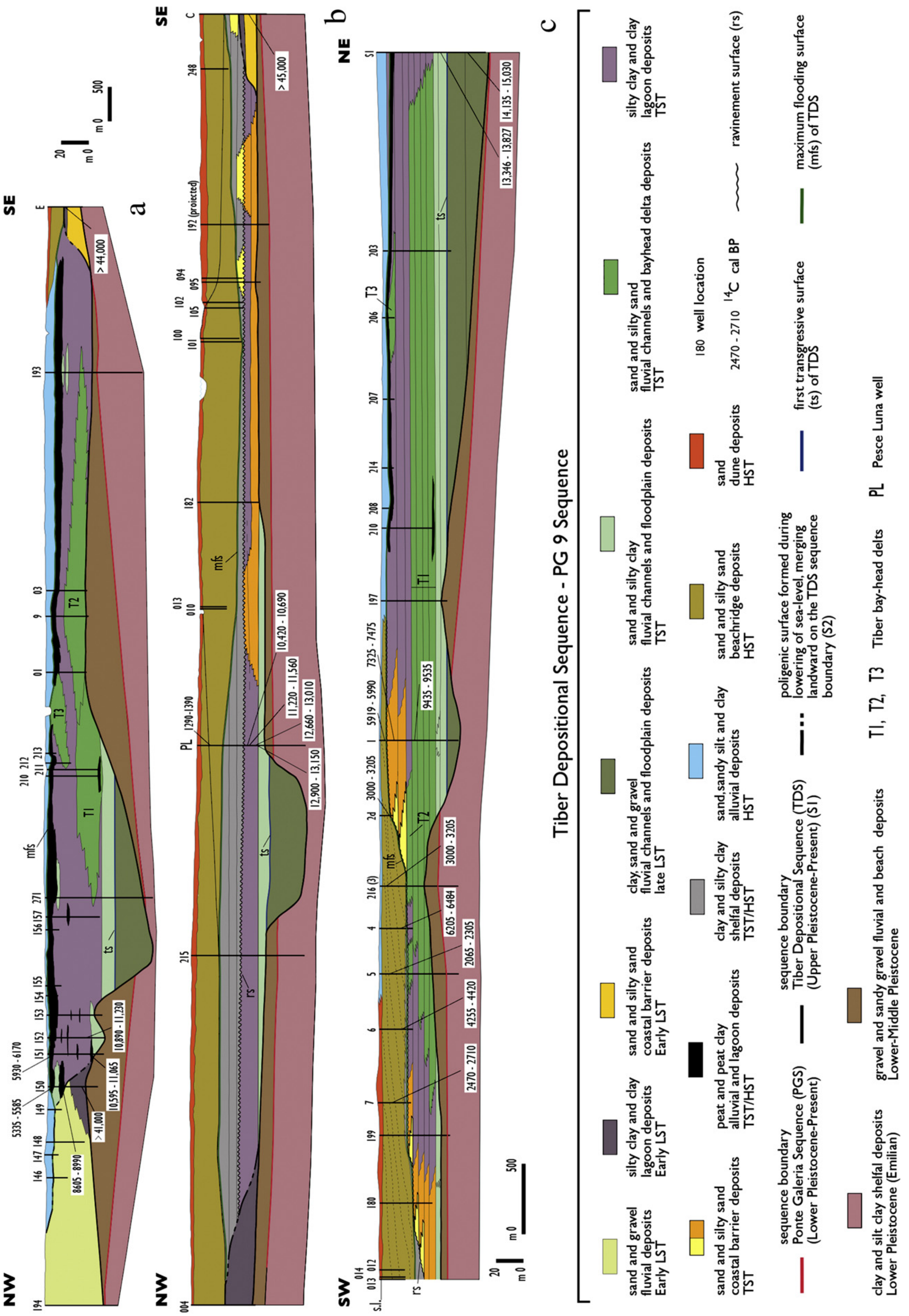

Fig. 9. Stratigraphic cross-sections of the Tiber Depositional Sequence. For tracks of cross-sections see Fig. 4.

ostracoda and foraminiferal assemblage (F3) is substantially similar to the previous one.

Both facies associations are interpreted to represent a shelf-transition zone, a sector extending from mean storm wave base to mean fairweather wave base, and as such is characterized by a typical alternations of high and low energy conditions (Reading and Collinson, 1996). The first facies association, with thin sand layers, represents the more internal sector transitionally passing to lower shoreface. This interpretation is consistent with the absence or the reduced presence of local fauna in some samples and the presence of shell debris with sandy layers that can be considered as the product of erosion and deposition phases respectively, related to storm events. However, it is not excluded that some of these sand layers were the result of flood events. The second facies association represents the more external sector, transitionally passing to inner shelf.

4.4.3. Inner shelf

The deposits related to this facies association develop between −21 and −17.90 m (Figs. 5 and 6; Table 1). They are constituted by a homogeneous bioturbated silty clay (Fig. 6f), which shows an assemblage with (F3) high species diversity dominance of *A. parkinsoniana*, *E. poeyanum* and miliolids as *Quinqueloculina seminulum*, *Q. stelligera*, and *Q. pygmaea*, species frequent in the infralittoral zone, mainly on vegetated bottoms (Cimerman and Langer, 1991; Langer, 1993; Sgarrella and Moncharmont-Zei, 1993). Subordinate species are *E. granosum*, *H. depressula* and *A. tepida*, which indicate a infralittoral environment affected by freshwater influence. The presence of *Bolivina* spp. and *Bulimina elongata* is coherent with the type of substrate characterized by muddy bottom with a high content of organic matter (Jorissen, 1988).

The ostracoda assemblage is dominated by *Palmoconcha turbida* and *Pontocythere turbida*, with subordinate *C. antiquata*, *L. ramosa* and *S. incongruens*: they are all marine infralittoral species (Pugliese and Stanley, 1991; Montenegro et al., 1998). No pollen was found in these deposits.

The sedimentological and micropaleontological data suggest for this facies association a relatively open-marine environment, below the storm wave base (inner shelf), and locally interested by the freshwater currents related to the near Tiber mouth.

4.4.4. Upper and lower shoreface

The deposits of this unit consist of two transitional facies associations developing between −17.90 and −2 m core depth (Figs. 5 and 6; Table 1). The first and lower facies association (between −17.90 and −8 m) consists of fine to very-fine sand with frequent intercalations of thin silty clay levels and widespread shell material (Fig. 6g). No ostracods and pollen have been found; the foraminiferal assemblage is characterized by normal marine infralittoral taxa such as *Ammonia* spp. and subordinately taxa as *Elphidium* spp. and miliolids (F3 assemblage). The second and upper facies association (between −8 and −2 m) consists of medium to fine sand with very rare silty clay intercalations (Fig. 6h). Very small shell and plant debris occur in this portion while no foraminifers, ostracods and pollen have been found.

The stratigraphic position of this deposits and their textural and microfaunistic composition allow interpreting the two facies associations as lower and upper shoreface deposits respectively. The absence of microfaunistic assemblages in the upper shoreface, and the presence of a reduced quantity of species in the lower shoreface is in agreement with this interpretation, a feature typical of the littoral environment where wave processes are very active. On the other hand the widespread shell and plant debris suggest a transport under high-energy conditions and probably a generalized migration of these materials through longshore currents. Based on this interpretation and taking into account the position of the Pesce Luna well, the above deposits can be attributed to the delta front of a prograding wave-dominated delta system.

4.4.5. Dune, interdune and foreshore deposits

This uppermost portion of core (0–2 m) has been strongly altered by human activity. Anyway, sediments are fine to medium and coarse sands, generally barren, with variable percentage of shell (pulmonata gastropodas and reworked littoral microfauna) and plant debris (Fig. 5). The sand is reddish yellow, rich in quartz and mica with variable quantities of heavy minerals. Tabular and trough cross-bedding are frequent as well as bioturbation due to roots. In general terms these sediments are part of the outer delta plain and constitute present and relict dune and interdune deposits in the uppermost part that transitionally passes downward to foreshore deposits.

5. The TDS Late Quaternary fourth-order depositional sequence

Based on the data derived from the Pesce Luna core and taking into account the literature data (Bellotti et al., 1994, 1995, 2007, 2009, 2011; Chiocci and Milli, 1995; Milli, 1997; Amorosi and Milli, 2001; Giraudi, 2004, 2011; Giraudi et al., 2009; Di Bella et al., 2011) we propose a detailed description of the stratigraphic architecture of the TDS, based on three correlation panels, one of which is oriented perpendicular to the present coastline and two are oriented parallel to it (Figs. 4 and 9). Such panels show how the stratigraphic succession below the present Tiber coastal plain can be subdivided into three units bounded by uncorformity surfaces.

The lowermost stratigraphic unit consists of clay and silty clay with local intercalations of sandy levels. The foraminiferal assemblage characterized by typical circalittoral benthonic taxa (*Bolivina* spp., *Bulimina* spp., *Cassidulina carinata*, *Melonis* spp., *Bigenerina nodosaria*, *Hyalinea balthica*, *Cibicidoides pachyderma*, *Gyroidina* spp., *Textularia* spp., *Hanzawaia boueana* and *Dorothia gibbosa*) and significant frequencies of planktonic species (*G. bulloides*, *Globigerina falconensis*, *G. ruber*, *Glorotalia inflata*, *Globorotalia oscitans*, *Glorotalia scitula*, *Neogloboquadrina pachyderma* and *Turborotalia quinqueloba*), suggests an offshore environment. The age of these deposits is attributed to Lower Pleistocene (Emilian stage, 1.2–1.5 Ma) by the presence of *H. balthica* (Carboni, 1993).

The middle stratigraphic unit is constituted by gravels and sandy gravels with pebbles of carbonate rocks from the Apennines and rare volcanic clasts derived from the volcanic complexes of the Roman Comagmatic Province. Such deposits crop out along the margin of the Tiber coastal plain and have been attributed, through a detailed facies analysis, to fluvial and beach environments (Bellotti et al., 1993; Milli, 1997). They are essentially Middle Pleistocene in age and belong to one of the high-frequency depositional sequence forming the PGS (Figs. 2 and 3).

The uppermost unit is represented by the TDS. This unit constitutes an incomplete fourth-order depositional sequence, which is still evolving. The lower boundary of this sequence is an erosional surface that cuts the underlying Lower and Middle Pleistocene deposits. The structural contour map of this unconformity (Fig. 4) shows raised and lowered areas, linked to the original structural situation and to phases of erosion which mainly occurred during the last glacial lowstand. The TDS sequence boundary began to form with the sea-level fall occurring after the last highstand phase correlated to the marine oxygen isotope stage (MIS) 5. The peak of this fall should coincide with the last glacial maximum expansion (LGM), and in particular with the most negative peak (between 19 and 17 ka cal BP) of MIS 2. Recently Lambeck et al. (2002) have defined "*the onset of the LGM as the time sea levels first approached their minimum levels at about 30,000 years ago*". Basing on this definition they suggest a duration of 10,000 years for the LGM (between 30 and 19 ka cal BP), a period during which ice volume increased very slowly and the eustatic LGM lowstand could have been as much as 135–140 m below present sea level. Differently from the previous Authors, Peltier and Fairbanks (2006) suggest that LGM must have started 26,000 years ago having a duration of about

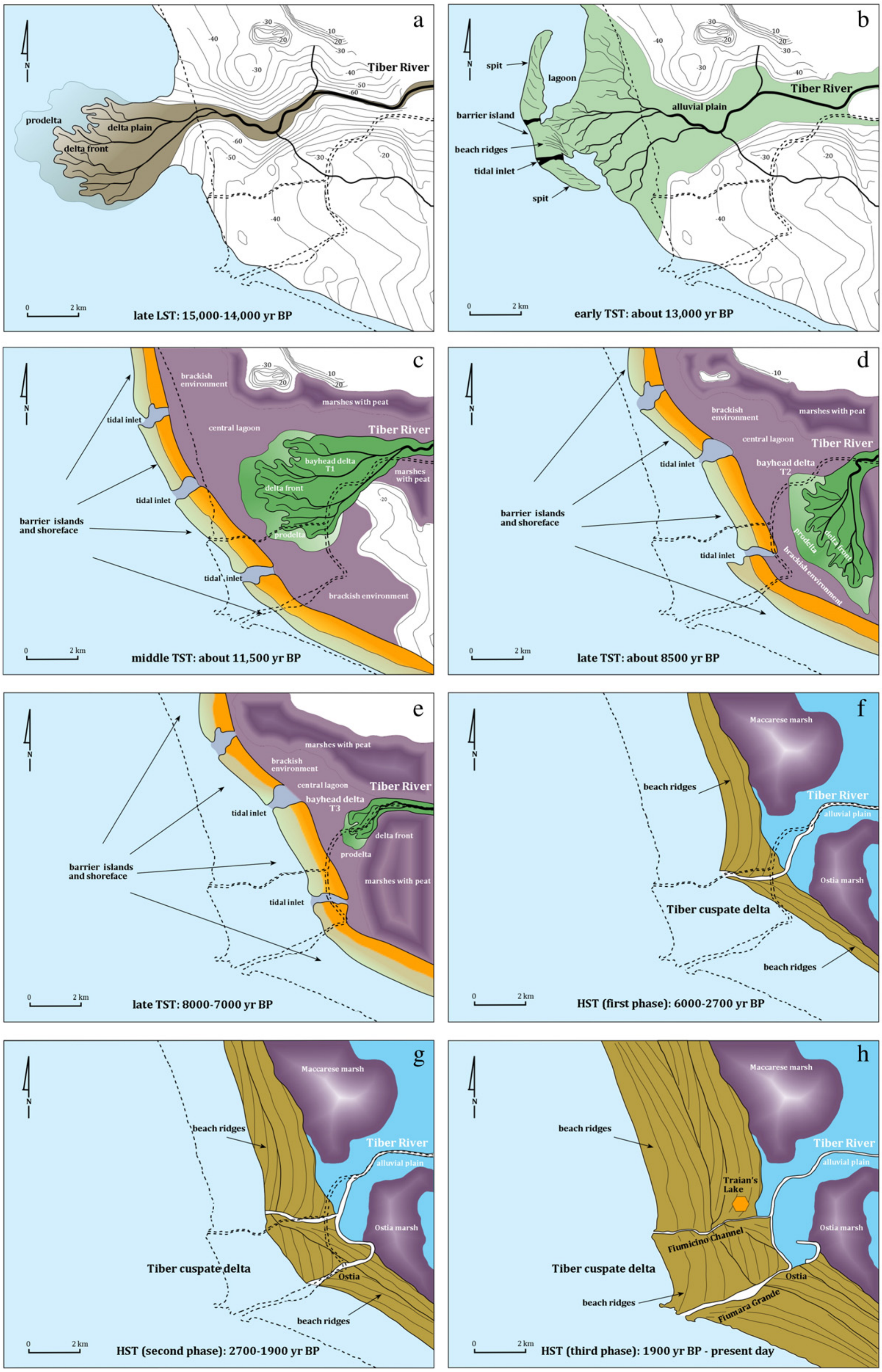
a
Tiber River
prodelta
delta plain
delta front
late LST: 15,000-14,000 yr BP
b
spit
lagoon
barrier island
beach ridges
tidal inlet
spit
alluvial plain
Tiber River
early TST: about 13,000 yr BP
c
brackish environment
marshes with peat
central lagoon
Tiber River
tidal inlet
bayhead delta T1
marshes with peat
delta front
tidal inlet
barrier islands and shoreface
prodelta
tidal inlet
brackish environment
middle TST: about 11,500 yr BP
d
brackish environment
marshes with peat
central lagoon
Tiber River
tidal inlet
bayhead delta T2
barrier islands and shoreface
tidal inlet
prodelta
delta front
brackish environment
late TST: about 8500 yr BP
e
marshes with peat
brackish environment
central lagoon
Tiber River
bayhead delta T3
tidal inlet
delta front
prodelta
barrier islands and shoreface
marshes with peat
tidal inlet
late TST: 8000-7000 yr BP
f
Maccarese marsh
beach ridges
Tiber River
alluvial plain
Ostia marsh
Tiber cuspate delta
beach ridges
HST (first phase): 6000-2700 yr BP
g
Maccarese marsh
beach ridges
Tiber River
alluvial plain
Ostia marsh
Tiber cuspate delta
Ostia
beach ridges
HST (second phase): 2700-1900 yr BP
h
Maccarese marsh
beach ridges
Tiber River
alluvial plain
Traian's Lake
Fiumicino Channel
Ostia marsh
Tiber cuspate delta
Ostia
beach ridges
Fiumara Grande
HST (third phase): 1900 yr BP - present day
2 km

5000–7000 years (between 26 and 19 ka cal BP); they also estimate the eustatic lowstand at about 120 m below present sea level. Regardless the onset of LGM both papers set the end of this period about 19,000 years ago, as from this date there was an initial melting of ice and a concomitant slow rise in sea level that lasted up to about 14,000 cal BP. In terms of sequence stratigraphy we correlate the end of the eustatic sea-level fall with the onset of the LGM (Early Lowstand Systems Tract, ELST) and the period of eustatic stillstand with the duration of the LGM. This latter period together with that related to the subsequent eustatic rise corresponds to the Late Lowstand Systems Tract (LLST).

Sedimentological and stratigraphic data suggest that the sea-level fall was punctuated by multiple higher-frequency (fifth-order) sea-level cycles, the stratigraphic record of which is only partially preserved below the present Tiber delta plain; they can be interpreted as the forced regressive deposits related to the ELST (*sensu* Posamentier and Allen, 1999) of the TDS. The most important element is the east–west oriented depression stretching from the coast up to the urban area of Rome, along a well-defined graben that coincides with the present course of the Tiber (Bellotti et al., 1994). This depression (Fig. 4), evidenced in the correlation panels (Fig. 9a,b), should continue also in the more internal portion of the continental shelf (we have no data available to confirm) and has been interpreted as the paloevalley (incised valley) of the Tiber River formed during the post-Tyrrhenian sea-level fall and partially reworked during the subsequent sea-level rise.

Based on what said above and taking into account the new data, a modification of stratigraphic framework of TDS is now suggested. Unlike previously suggested by the literature data (Bellotti et al., 1994, 1995; Chiocci and Milli, 1995; Amorosi and Milli, 2001), beneath the Tiber delta plain, the deposits are not only attributed to the transgressive and highstand systems tracts, but also to the early and late lowstand system tracts. This allows to consider the TDS as one of the most complete late Quaternary high-frequency depositional sequences in the Mediterranean area, although the major thickness of sediments beneath the present Tiber delta plain consists almost entirely of a transgressive–regressive wedge formed during the last 14,000 years.

5.1. Lowstand system tracts

On the basis of our data and taking into account previously published material from the Mediterranean area (see Coutellier and Stanley, 1987; Hernández-Molina et al., 1994; Stanley and Warne, 1994; Amorosi and Milli, 2001; Boyer et al., 2005; Labaune et al., 2005) the lowstand deposition in the Tiber area took place between 120 and 14 ka cal BP (from the beginning of substage 5d to the final phase of stage 2). Because of this complex process the preservation of the deposits formed during the sea-level fall is very low, whereas the deposits formed during the stillstand and initial sea level rise are largely preserved. The new data from Tiber area allow to differentiate the deposits formed during the sea level fall (early lowstand) from those formed during the stillstand and initial sea level rise (late lowstand). Correlation panels (Fig. 9) show both these types of deposits evidencing two important surfaces (S1 and S2) bounding below and above these units, respectively.

The surface below the forced regressive deposits (S1) is considered to represent the master sequence boundary unconformity (*sensu* Posamentier and Allen, 1999) of the TDS; it formed due to the fluvial incision following the episodic relative sea-level fall, a mechanism that seems to characterize both the falling and rising sea level phases during the Quaternary. The S1 surface extends well beyond the area interested by this study, being this unconformity placed at the base of the last post-Tyrrhenian glacial–interglacial cycle. It has been recognized along the entire Tyrrhenian margin of the Italian peninsula both landward and seaward (see Chiocci et al., 1997; Chiocci, 2000; Aguzzi et al., 2007; Amorosi et al., 2008, 2011).

The surface above the forced regressive deposits (S2) constitutes a polygenic erosional unconformity always forming during the episodic relative sea-level fall and merging landward with the PG9/TDS sequence boundary. In the latter area these surfaces, together, constitute the base of the Tiber incised valley in the depocenter sector of the basin (Fig. 9). The geometric features of Tiber incised valley show many of the characters recognized in other Quaternary valleys and in experimental studies: the basal valley-fill surface develop from multiple episodes of incision and channel-belt formation during relative sea-level fall (Blum and Price, 1998; Blum and Törnqvist, 2000; Blum and Aslan, 2006). Besides, the incised valley is wider than the surface valley that created it (Fielding and Gibling, 2005; Gibling, 2006; Sheets et al., 2007), and the valley widens downstream due to increases in sediment flux from valley excavation (Strong and Paola, 2008; Martin et al., 2011). The Tiber valley, from landward to seaward, shows a different geometry, which probably reflects not only the dynamics of erosive process, but also an influence of tectonic lineaments related to the extensional tectonics that interested the Latium Tyrrhenian margin starting from the Upper Miocene.

The preserved early LST deposits (between 120,000 yr and 30,000–26,000 yr BP) occur in the northernmost and southernmost part of the investigated area and are constituted by fluvial, lagoonal and beach deposits. Fluvial deposits are characterized by different lithofacies ranging from sand and gravel, to mud and travertine. Such deposits are organized in fining-upward facies sequences that are interpreted as the filling of low-sinuosity channels of a braided fluvial depositional system. In particular sands and gravels should have constituted bars bodies that filled the channels while the mud, also for the presence of pulmonata gastropoda fauna, is interpreted as a flood plain deposits. As a whole these fluvial deposits form a sedimentary body with a tabular geometry that extends over 3–5 km with a thickness between 10 and 30 m. Beach deposits are constituted by gravels and sandy gravels forming coarsening upward facies sequences. When preserved such sequences show an overall passage from lower and upper shoreface (the fauna includes a few benthonic foraminifera as *Lobatula lobatula*, *A. parkinsoniana*, *Asterigerinata mamilla*, and *Elphidium* spp.) to foreshore (with a few foraminifera, plant debris and shell fragments), and finally a backshore facies (with plant debris and pulmonata gastropods). Lagoonal facies are constituted by organic-rich mud deposits with frequent intercalations of thin sandy layers, often associated to shell debris. Four radiocarbon dates were obtained from the peaty mud deposits occurring in the lagoonal deposits, confirming an age older than 40,000 years BP (see Bellotti et al., 2007).

The late LST deposits, (age between 30,000–26,000 yr and 14,000 yr BP), about 24 m thick, occupy the most depressed area (valley axis) of the Tiber incised valley. This means that during the late LST sedimentation the TDS sequence boundary unconformity was in subaerial conditions. The valley fill is constituted by fluvial sandy and sandy gravels deposits passing laterally and vertically to floodplain muddy deposits with peat layers. Gravels are represented by heterometric carbonate and chert clasts, less 10 cm in diameter, ellipsoidal or spherical in shape, which are derived by the erosion of the Lower and Middle Pleistocene fluvial and beach deposits cropping out along the margins of the present Tiber delta plain. During the late LST sedimentation the Tiber River flowed in ENE–WSW direction,

Fig. 10. Paleogeographical sketches showing evolution of the Tiber River during the last 18,000 yr BP. a) late lowstand systems tract; b, c, d, e) transgressive systems tract; f, g, h) highstand systems tract. The colors in the figure identify the different depositional environments (see the labels) developing during the systems tracts.

1–5 km north of its present location, and 80–85 m below the present topographic surface. At that time, the Tiber was fed by a tributary which ran parallel to the present shoreline (Figs. 9c and 10a).

In our interpretation these fluvial deposits (calibrated radiocarbon dates indicate for these deposits an age of 14,135–15,030 yr BP) that constitute the uppermost portion of the late LST deposits, should pass seaward to the late lowstand Tiber deltaic body that developed during the stillstand and slow sea-level rise phases characterizing the late LST (Fig. 10a). This deltaic body was probably located about 8–10 km from its present position, at the end of the incised valley where it merges into the basal unconformity (TDS sequence boundary) at a depth between −80 and −110 m below the present sea-level (outer shelf area) (see also Bellotti et al., 1994). The reconstructed stratigraphy of the late LST allows to differentiate a lower and an upper portion, the first being characterized by fluvial and delta progradation and the second by fluvial and delta aggradation. This change in depositional trend of late LST deposits is related to the increase of sea-level rise rate, although this effect is amplified by the local confinement of the incised valley (see also Posamentier and Allen, 1999). The aggradation phase constitutes the prodrome to the true transgressive phase and is characterized by an assemblage of sandy fluvial and muddy and peat muddy alluvial deposits with widespread organic matter and shell debris (pulmonate gastropode).

We have no data about the vegetation assemblage in the Tiber area during the Late LST. A marine pollen record from the Bay of Salerno (Russo Ermolli and di Pasquale, 2002) and a lacustrine record from the Roman plain (Follieri et al., 1988) suggest that the vegetational landscape of the Tyrrhenian coast was herb-dominated, with modest presence of deciduous trees, mostly *Quercus*.

5.2. Transgressive Systems Tract

In the Tiber area the TST is constituted by the deposits accumulated between 14 and 5–6 kyr BP. Such deposits lie directly on the basal unconformity and below the present delta plain form almost the whole of the TDS. As evidenced by Bellotti et al. (1994, 1995) and Amorosi and Milli (2001) these deposits show a facies distribution and a stratal architecture characterized by a retrogradational stacking pattern of the depositional systems, which include from landward to seaward: a fluvial-bay-head deltaic system, a coastal barrier-lagoon system and finally a transition to shelf system. The complex interfingering between these depositional systems was the response to the onset of the transgression and the concomitantly transformation of the Tiber incised valley into a wave-dominated estuary (Amorosi and Milli, 2001; *sensu* Dalrymple et al., 1992; Nichol et al., 1994; Boyd et al., 2006), a depositional setting also recognised in the late-glacial and Holocene transgressive succession characterizing other Mediterranean deltaic systems (see Amorosi et al., 2004, 2005 for the Po delta; Aguzzi et al., 2007; Amorosi et al., 2008, 2011 for the delta systems along the Tuscan coast of Italy; Somoza et al., 1998 for the Ebro delta; Boyer et al., 2005; Labaune et al., 2005 for the Rhône delta).

More in detail the TST deposits are organized in small-scale (m-thick) shallowing-upward cycles (parasequences) showing characteristic facies sequences as a function of relative position within the estuary (Bellotti et al., 1994, 1995; Amorosi and Milli, 2001 for a more detailed description of these cycles). A very interesting aspect is also the relationship between the vertical facies framework recognized in these cycles and the vegetation history, as recognised by Aguzzi et al. (2007), Amorosi et al. (2008) and Amorosi et al. (2005) in the transgressive successions of the Arno and Po deltas respectively. In the Tiber delta the paleoclimatic characters related to this transgressive phase are well-marked through the pollen and plant macroremains records from Pesce Luna, recording the late-glacial vegetation of a coastal area. The vegetational landscape was characterized by major environmental shifts, affecting both composition and structure of the vegetation, as it commonly occurs in estuarine environments (Bellini et al., 2009; Di Rita et al., 2010; Di Rita and Magri, 2012).

The transgressive cycles characterizing the TST are thought to be the response to a discontinuous relative sea-level rise that was punctuated by stillstand or quasi-stillstand phases during which depositional systems experimented short phases of progradation. This mechanism, characterized by acceleration and deceleration of sea-level rise, may be related to a discontinuous increase of freshwater derived from melting of continental ice (meltwater pulse, MWP) superimposed on the overall sea-level rise (Bard et al., 1996, 2010). In the Mediterranean area two maxima in the sea-level rise rate, corresponding in terms of climatic variations to intervals of rapid warming and melting of continental ice, have been recognised in the post-glacial sediments of the central Adriatic sea (Asioli et al., 1996; Trincardi et al., 1996; Cattaneo and Trincardi, 1999), of the Po delta (Amorosi et al., 2004), as well as of the Rhône delta (Berné et al., 2003; Boyer et al., 2005). These intervals are separated by a cool climatic episode coincident with the Younger Dryas (YD). Bard et al. (2010) indicate for the periods of rapid sea-level rise values of 12.1 ± 0.6 mm/year and 11.7 ± 0.4 mm/year before and after the YD respectively. A slowdown of sea-level rise should characterize the YD having values of 7.5 ± 1.1 mm/year.

Based on the previous considerations the depositional architecture within the TST of TDS can be subdivided into a series of steps recording the sedimentary evolution of the study area, which reflect the interplay between relative and discontinuous sea-level rise, and the variation of sediment supply, modulated by the concomitant climatic changes.

During the early phase of TST (between ~14,000 and 13,000 cal BP), due to the rapid sea-leve rise the late lowstand Tiber deltaic body was rapidly drowned and reworked, probably according to the transgressive submergence model of Penland et al. (1988) (Fig. 10b). On top of the delta a distinct erosional surface was formed. It represents the transgressive surface separating the lowstand from the transgressive systems tract (Posamentier and Vail, 1988; Posamentier and Allen, 1999). In the marine sector such surface was produced through the wave erosion of the upper deltaic body, and is called also wave-ravinement surface (Swift et al., 1972; Swift, 1975). Landward, the same transgressive surface separates the underlying Late LST fluvial and flood plain deposits from the overlying TST fluvial and flood plain deposits. During this phase, the Tiber River flowed into the sea again, and the deltaic body, due to the rapid rise in sea level was transformed into an "erosional headland with flanking barriers" (Penland et al., 1988), at the back of which open lagoons occurred (Fig. 10b).

A pollen record from the Roman plain (Di Rita et al., 2012) points to the development of an open woodland with mainly deciduous trees, in a period characterized by fluctuating climate conditions, substantially warmer and wetter than in the LGM.

Between 13,000 and 11,500 cal BP after the initial and rapid sea-level rise a slowdown occurred during the cold period of the Younger Dryas. With the progressive submersion of the Tiber incised valley, the new-formed barrier-island migrated landward, a lagoonal basin developed extending further in NW–SE direction and the Tiber river began to form the bay-head delta T1 that was active until approximately 9200 yr BP (see also Bellotti et al., 1994), although its final sedimentation phase was coeval with the deltaic body T2 (Fig. 9a,c).

During the initial sea-level rise phase an avulsion process occurred within the incised valley and the Tiber River migrated its course toward SE of about 2.5 km with respect to the previous position. The new-formed T1 delta was very close to the barrier island and both remained in a stable position. With the deceleration of sea-level rise during the YD, there was a probable increase of sediment supply that allowed a stabilization of both depositional systems. Sea water invaded the outer part of the bay-lagoon, while in the inner part a freshwater environment predominated (Fig. 10c).

T1 delta shows in strike section a lenticular geometry, has a maximum thickness of 20–21 m and extends laterally for about 3 km. The paleogeographic setting suggests that it can be considered as a river-dominated delta having a subaerial delta plain, a delta front with a subaqueous mouth bar, and a prodelta slope. The lagoonal basin, the sector with the lowest energy, constituted the prodelta region of the bay-head delta. In this sector peat, and other organic matter deposits were present at different stratigraphic levels.

Microfaunistic and vegetation data support such interpretation (Facies association B). The foraminiferal and ostracoda assemblages indicate a brackish lagoonal environmment. Pollen data suggest that between 13,000 and 12,200 cal BP the succession of xerophytic herbs (mainly Cichorioideae and Chenopodiaceae), followed by grasses, *Juncus-Carex-Typha* communities, and aquatics, indicating a progressive rise of the water table in a newly formed freshwater basin, occurred. In the landscape surrounding the Tiber delta area, an open deciduous woodland, accompanied by increasing amounts of evergreen elements, was found, consistently with the vegetation features recorded in other sites of the region (Di Rita et al., 2012 and references therein). Around 12,000 yr BP the arboreal vegetation underwent a clear reduction of broadleaved trees, an important development of *Pinus*, and an appreciable increase in xerophytes. These vegetational changes were most likely determined by climate conditions unsuitable for trees, coeval with the global Younger Dryas fluctuation. The general features of this late-glacial opening of the vegetation at Pesce Luna are in good agreement with the vegetation dynamics observed in other pollen records of the Latium region (Magri, 1999; Di Rita et al., 2012), although xerophytes are much less abundant in the coastal areas than inland. Plant macroremains reveal that the wetland underwent a lowering of the water level with exposure of sandy soils.

The final phase of the TST developed between 11,500 and 6000–5000 yr cal BP. After the deceleration of sea-level rise characterizing the YD, a new acceleration phase occurred until 9000 yr BP, followed by a new decrease rate of sea-level rise, documented in the whole Mediterranean area (see Bard et al., 2010). This led to a rapid landward migration of barrier island and Tiber bay-head deltas. T1 delta was active until ~9000 yr BP, then it was abandoned and a new deltaic body (T2) was formed in the southeastern portion below the present delta plain (Fig. 10d). T2 delta shows a lens-shaped geometry in strike section, has a maximum thickness of about 17–18 m and extends laterally for about 5.6 km (Fig. 9a). This major lateral extension is thought to be the response to a decrease in the rate of sea-level rise and, consequently, to a minor accommodation space; T2 delta was active until approximately 8500 yr BP.

The last sea-level rise phase that precedeed the cold climate event of 8.2 yr BP (Barber et al., 1999; Clarke et al., 2004), coincides with a global eustatic jump estimated about 3 ± 1.25 m (Hijma and Cohen, 2010). This rapid sea-level rise and the further reduction of accommodation space caused, in our interpretation, a new avulsion of the Tiber river and the formation of the bay-head delta T3 (Fig. 10e), which developed during a period of deceleration of sea-level rise related to the cold 8.2 yr BP event. A similar evolution is common to other modern delta systems (see Bird et al., 2007; Hori and Saito, 2007; Tamura et al., 2009).

The T3 body is smaller than T1 and T2 (1.4 km in lateral extent) and reaches a thickness of 5–10 m (Fig. 9a,c). It prograded very rapidly within the lagoon, reached the coastal barrier, and flowed into the sea, giving rise to the initial construction of the present-day wave-dominated delta, an evolutive process developing during the subsequent highstand systems tract.

The final sedimentation phase of TST is marked into the lagoon by the presence of a thick and continuous peat layer, dated between 6000 and 5000 cal BP (Fig. 9a,c). The formation of this layer, similar to that recognised in the Rhine-Meuse delta (this delta has extensive peat formation between ~6000 and ~3000 cal BP, see Gouw and Erkens, 2007), is thought to be produced when sediment supply to the delta was insufficient and the available accommodation space was filled by peat, which grew during the very slow rise of groundwater table in turn related to the very slow rise of eustatic sea-level (see Van Asselen, 2011). It is not a coincidence that this process occurred in this period of time. The formation of the peat layer coincides, in fact, with the maximum transgression phase that closed at the top the TST of TDS with the maximum flooding suface (*mfs*) (Fig. 9). Landward this surface is placed on top of the peat layer. Seaward it is placed within the condensed section that represents the time of maximum flooding on the shelf. On the shelf in front of the Tiber river, the condensed deposits have been recognised on high-resolution seismic profiles as an acoustically transparent unit lying directly on the TDS sequence boundary (Bellotti et al., 1994; Chiocci and Milli, 1995).

In the Pesce Luna well (Fig. 5) the *mfs* is present within the inner shelf silty clay deposits that close the clear transgressive trend recognized in the TST in the passage from estuary to marine depositional system (-48 m to $-19/-20$ m). As shown in the correlation panel (Fig. 9b), the *mfs* is placed at different depths. Such character is strictly related to the fact that the time of maximum transgression in a basin is a function of the local sediment supply with respect to the local rate of relative sea-level rise (Wehr, 1993; Allen and Posamentier, 1994; Martinsen and Helland Hansen, 1994; Posamentier and Allen, 1999). Consequently the maximum flooding surface can be a diachronous surface in a depositional strike section and assumes the significance of a chronostratigraphic surface in a dip section as shown in the correlation panels (Fig. 9b,c).

From the microfaunistic point of view the TST sedimentation, between 11,500 and 5000–6000 cal BP, is characterized by foraminiferal and ostracoda assemblages, which indicate a passage from brackish, lagoon–marsh to brackish-marine and finally marine environments. Pollen analysis suggests that at the onset of the Holocene the marked reafforestation process widely recorded in the region (Magri, 1999; Drescher-Schneider et al., 2007; Di Rita et al., 2012) was overshadowed by the local development of an unstable environment with marshes, swamps, ponds and wet meadows occurring under the influence of a rapid rise of the sea level. A mixed deciduous woodland developed, a feature also recognized by Amorosi et al. (2004), and Aguzzi et al. (2007) and Amorosi et al. (2008) in the Late Quaternary Po and Arno coastal plain deposits respectively. The evergreen coastal vegetation underwent a steady increase. The riparian vegetation became part of the local coastal and estuarine environment, as it still occurs at present. Around 10,400 yr cal BP, a marked reduction of the wetland in favour of sandy soils and a brackish environment suggests that the sea was near. A stable arboreal vegetation formed, characterized by a deciduous coastal forest with progressive increase in evergreen elements. This landscape persisted until the end of the record (ca. 9000 cal BP) and even later, as shown by the nearby sequence from Lingua d'Oca-Interporto (Di Rita et al., 2010).

5.3. Highstand Systems Tracts

The HST developed from 6000 to 5000 yr BP, when the sea level rise decreased to about 1 mm yr^{-1} (Bellotti et al., 1995, 2007) approaching a relatively stable position. The filling of the lagoon formed during the TST and the subsequent cuspate delta formation were the dominant features of the Tiber area. Within this lagoon the bay-head delta T3 prograded very rapidly due to the increase of sediment supply and the decrease of the rate at which new accommodation space was created. The lagoon was transformed into two marshy coastal ponds (Stagno di Maccarese to the north and Stagno di Ostia to the south), poorly and intermittently connected to the sea, which remained active up to the 1884 reclamation (Amenduni, 1884). The most recent data (Giraudi, 2004, 2011; Bellotti et al., 2007, 2011; Giraudi et al., 2009; Goiran et al., 2009; Di Rita et al., 2010; Di Bella et al., 2011) show a very complex paleoenvironmental evolution of the Tiber river over the last 6000 years and indicate that major environmental changes were largely induced by climate and subordinately by human impact.

Such evolution can be subdivided into three different phases (Fig. 10f,g, h) (see also Bellotti et al., 2011).

At the beginning of the first phase, (6000–2700 cal BP) (Fig. 10f), the Tiber acquired a marine mouth after the progradation of bay-delta T3 within the lagoon (approximately between 7000 and 6000 cal BP). A cuspate delta with several beach ridges (strandplain) dated to 6000–5700 cal BP (see also Giraudi, 2004; Bellotti et al., 2011), was built over the area stretching from the present Capo due Rami to the site where the Trajan Imperial harbor was subsequently built. The landward margin of this strandplain marks both the innermost limit of the transgressive coastal barrier and the starting point of the first highstand of the Tiber marine delta progradational phase. During this phase, lasting about 3000 years, the Tiber prograded at a rate of at least 1 m/year. Pollen analysis (see Bellotti et al., 2011) suggests that toward the end of this phase the landscape was covered by a mixed oak-dominated woodland with evergreen elements. In particular, starting from 3000 cal BP, a spread of arboreal vegetation characterized by evergreen and deciduous *Quercus* with *Juniperus* suggests the expansion of forest communities on the newly available land produced by the cuspate delta accretion. From the historical point of view the transition from the first to the second phase, in the 7th century BC, was contemporary to the foundation of ancient Ostia, as suggested by historical accounts (cf. Bellotti et al., 2011).

In the second phase (Fig. 10g), between 2700 and 1900 cal BP, an abrupt southward migration of the river mouth occurred, probably as a result of a strong flood event. This event occurred during a cold climatic phase recognized in the Mediterranean area (Incarbona et al., 2010) and coincident with the Bond cycle B2 (Bond et al., 1997). The Tiber river flowed into the Ostia pond, thereby opening a new mouth about 3 km south of the previous one (the present Fiumara Grande mouth).

At the mouth of this new channel the Tiber river began to build a new lobe while the old one no longer fed was subject to erosion. The intrusion of sea water into the marshy coastal Ostia pond is highlighted by a peak of foraminiferal lining, a change in the mollusc record, the appearance of *Ruppia* and an increase in Chenopodiaceae. The cuspate delta advanced seaward very quickly so that, about 2350–2400 cal BP, it was almost fully developed. The mouth progradation rate was estimated to be about 5–6 m/year. After this phase the growth of the delta was interrupted by a new erosive process that produced the erosion of the beach ridge and the apex of the delta as suggested by the reconstruction of the shoreline (γ line in Bellotti et al., 2011), which has a gently curved shape. According to recent data (Bellotti et al., 2011; Giraudi, 2011), this erosive process occurred about 1650 cal BP (third century AD) during the Roman Warm Period that was characterized by a decrease of Tiber floods. From 2400 yr BP onwards, the human influence played an important role on the natural landscape and the presence of significant amount of cultivated and anthropochore plants suggests an intensive exploitation of the area by human communities, particularly during the Imperial times.

At the beginning of the third phase (Fig. 10h) (from about 1900 cal BP to present day), the Tiber progradation gave rise to a complex cuspate delta built up by two distributary channels that were almost simultaneously active: Fiumara Grande, the most important and natural distributary channel, and Fiumicino channel, dredged during the 1st century AD for the construction of the Roman Imperial Port. This phase corresponds to the last progradation of the Tiber delta, a process that has been quite intense over the last 500 years. During this period the Tiber delta experienced alternating phases of progradation, stability and erosion under the control of rapid climatic changes. This produced also the opening and the closure of the tidal inlet connecting the internal marshes to the sea, a mechanism strictly related to the evolution of the delta and in particular to the formation and lateral migration of the spits. It is worth noting that during this period of time there was a strong correlation between the Tiber flood events and the progradational phases of the delta, while the erosion of beach ridges occurred during phases with reduced sediment supply (Bellotti et al., 1994, 2011; Giraudi, 2011). Anyway, no variations of the shoreline position seem to have occurred between the 1st century and 1400 AD. Starting from the middle of the 15th century and until 1900 AD a major seaward shift in the shoreline position was recorded in coincidence with the Little Ice Age, when more frequent and intense floods are historically documented in the city of Rome. During this period the Tiber delta prograded for about 3 km at a rate of about 9 m/year (Bellotti et al., 1994; Giraudi, 2011). The same phase, with similar characteristics but different progradation rates, was recorded in other deltas of the eastern Tyrrhenian Sea (Caputo et al., 1987; Alessandro et al., 1990; Bellotti, 2000).

From the stratigraphic point of view the architecture of the HST is characterized by the development, in recent times, of a wave-dominated arcuate delta, with lateral transition to strandplains fed by longshore drift. Beneath the present delta plain, near the mouth delta, the evolutive trend of the HST deposits was characterized by a sand-dominated coarsening-upward facies succession produced by the progradation of the delta front onto prodelta clay/sand alternations (Figs. 5 and 9b,c). A similar trend has also been recognized for the deposits beneath the lateral strandplain (see other similar description in Coleman and Wright, 1975; Bhattacharya and Walker, 1992; Reading and Collinson, 1996; Bhattacharya, 2006). Seaward, HST deposits were observed with high-resolution seismic profiles. Such deposits are characterized by high-amplitude continuous internal reflections with subparallel internal configurations and downlap terminations; they tend to smooth the preexisting morphology, filling the depressions and smoothing the high (Bellotti et al., 1994).

A detailed examination of the cores regarding the cuspate delta and the lateral beach ridge formed during the three phases of HST, reveals that the stratigraphy of the cores shows a cyclic grain-size variation and an alternation of beach and lagoon (from open to closed) environments, which has been interpreted as the expression of the lateral variability of these sandy bodies, a character closely related to their different accretion mode. As shown in Fig. 10h, the beach ridges are more or less equally distributed on both sides of the mouth and as such the Tiber delta can be considered a symmetric wave-dominated delta (*sensu* Bhattacharia and Giosan, 2003). This character has been preserved during the evolution of the delta in the last 6000 years. However, until about 2700 BP, with the deltaic progradation the forming beach ridges gave rise to amalgamated sand bodies, about 20 m thick, with a clear coarsening-upward trend. This regular and symmetrical distribution of beach ridges on both side of the mouth suggests that the main wave directions were basically from the west sectors. Only the waves coming from these sectors would be able to redistribute the river load on both sides of the mouth. Since 2700 BP the beach ridges show an initial development towards the northern sectors, suggesting that in addition to the wave directions from the west, a wave direction from the south began to be more influent. The latter would have produced a weak northward littoral drift responsible of the slight asymmetry visible in the Tiber delta.

Another change concerns the mechanism of beach ridges accretion. Unlike earlier stages, the beach ridges that developed over the past 2700 years were not amalgamated, but were separated by muddy deposits that contain organic material and a fauna indicating a brackish environment, such as lagoons, or a slightly confined infralittoral environment affected by freshwater influence (Di Bella et al., 2011). These elements suggest that these sand bodies were originally barrier-spit systems, whose formation and evolution may follow the mechanism proposed by Bhattacharia and Giosan (2003), Giosan et al. (2005), van Maren (2005), Giosan (2007) and Dan et al. (2011). This mechanism emphasizes a close interaction between flood events, transporting large volumes of sediment to the subaqueous delta, and the waves, especially the storm waves, that may have reworked back this sand towards the shoreline (see also Rodriguez et al., 2000). The latter process would generate, over time, sand bodies attached to the delta mouth, which formed emergent and elongate shore-parallel sandy barrier-spits at the back of which, in more sheltered areas, fluvial and lagoonal deposits occurred. The barrier-spits would be attached with their downdrift tip to the mainland through the along- and cross-shore sediment transport. A consequence of this process was the transformation of the lagoonal basins into brackish coastal lakes and then into freshwater marshes. These were eventually covered by dune and interdune deposits, constituting the last evolutionary phase of the Tiber delta.

6. Conclusions

The integration of sedimentological, micropaleontological, and paleobotanical analyses coupled with radiocarbon data, allowed to unravel the complex evolution of the Tiber delta sedimentary succession deposited during the last glacial–interglacial cycle (last 120 ka) constituting the Tiber Depositional Sequence (TDS).

Facies and paleoenvironmental analyses together with the reconstructed stratigraphic architecture of this succession allowed a better sequence-stratigraphic interpretation of these deposits, which contain, with different thicknesses and details, the early and late lowstand, the transgressive and the highstand systems tracts.

This study confirms the lithofacies distribution resulting from transgression and infilling of a wave-dominated estuary, but also shows some important elements seldom described in the literature: 1) the local preservation of landward forced regressive deposits and their position within the Tiber incised valley, as well as their stratigraphic relationships with the adjacent systems tracts; 2) the infilling of the deeper portion of the incised valley with fluvial late lowstand deposits; 3) the good preservation of the barrier islands formed during the transgressive sea-level rise, that are rarely preserved, being removed by shoreface ravinement; this suggests a high accommodation during the TST; 4) the completeness and thickness of the preserved succession showing the transitional passage from a wave-dominated estuary to a wave-dominated delta with the increase of fluvial power, during the transition from transgressive to highstand conditions. This feature is rarely preserved in the ancient incised valley-systems (*sensu*, Zaitlin et al., 1994; Boyd et al., 2006).

Our study documents that the stratigraphic organization of TDS is the result of the interaction between global eustatic variations and sediment supply, both processes being under the control of climatic changes. The land subsidence, although present, may be considered negligible, in order to evaluate the variations in time and space of accommodation space. Land subsidence due to peat compaction can locally influence the sedimentation pattern through the generation of local accommodation space within which autocyclic facies sequences can be formed.

The recognised evolutionary trends evidence a deposition of alluvial and coastal systems during the regressive forced phase related to the eustatic sea-level fall between about 120 and 30–26 yr BP (early lowstand). With the subsequent stillstand and slow eustatic sea-level rise (late lowstand), a prograding delta and an aggrading incised-valley fluvial fill occurred. The Tiber incised valley was transformed into a wave-dominated estuary during the transgressive phase (TST), whereas subsequently a coastal-shelf sedimentation took place during the highstand phase (HST). Changes in sediment input, climatic variations and more recently, human activities played a major role in the development of the Tiber delta during the last 20,000 yr BP. This is well-evidenced by foraminiferal and ostracoda assemblages, as well as by vegetation assemblages (pollen and plant macroremains), which record the paleoenvironmental evolution of the study area in response to sea-level and climatic changes and, in the last thousands of years, to the influence of human activity. In recent times (last 3000 years) a strict relationships between progradational phases of the delta and flood events of the Tiber river has been evidenced, suggesting also an evolution of this last phase through the formation and merging of barrier-spits to the mainland, as recognized by other authors in similar settings.

Acknowledgements

Many individuals and organisations have supported the research on Tiber Delta. Financial support was provided by MIUR (Ministero Istruzione Università Ricerca), SAPIENZA University of Rome, CNR (Consiglio Nazionale delle Ricerche) and “CARG Project – Geological Map of Italy 1:50,000. We are very grateful to the ANAS for the access to core data. We would like to thank the two reviewers G. Sarti and L. Giosan, and the editor of Sedimentary Geology, Gert Jan Weltje for the critical review of the manuscript and for their positive comments and recommendations, which helped us to improve it.

Appendix A. Supplementary data

Supplementary data to this article can be found online at http://dx.doi.org/10.1016/j.sedgeo.2012.12.003.

References

Aavad, J.B., 1994. Bloom formation of Gloeotrichia echinulata and Aphanizomenon flos-aquae in a shallow, eutrophic, Danish lake. Hydrobiologia 289, 193–197. http://dx.doi.org/10.1007/BF00007420.

Aguzzi, M., Amorosi, A., Colalongo, M.L., Ricci Lucchi, M., Rossi, V., Sarti, G., Vaiani, S.C., 2007. Late Quaternary climatic evolution of the Arno coastal plain (Western Tuscany, Italy) from subsurface data. Sedimentary Geology 202, 211–229.

Alessandro, V., Bartolini, C., Caputo, C., Pranzini, E., 1990. Land use impact on Arno, Ombrone and Tiber deltas during historical times. In: Qnélennec, R.E., Ercolani, E., Michon, G. (Eds.), Littoral 1990, Eurocoast, Château-Gombert, Marseille (France) 9–13 July 1990, pp. 261–265.

Allen, G.P., Posamentier, H.W., 1994. Transgressive facies and sequence architecture in mixed tide-and wave-dominated incised valleys: example from the Gironde Estuary, France. In: Dalrymple, R.W., Boyd, R., Zaitlin, B.A. (Eds.), Incised valley systems: origin and sedimentary sequences: SEPM (Society for Sedimentary Geology), Special Publication, 51, pp. 225–240.

Amenduni, G., 1884. Sulle opere di bonificazioni della plaga litoranea dell'Agro Romano che comprende le paludi e gli stagni di Ostia, Porto, Maccarese e delle terre vallive di Stracciacappa, Baccano, Pantano e Lago dei Tartari. Relazione del progetto generale 15/7/1880. Min. LL.PP. Eredi Botta, Roma, pp. 1–36.

Amorosi, A., Colalongo, M.L., 2005. The linkage between alluvial and coeval nearshore marine successions: evidence from the Late Quaternary record of the Po River Plain, Italy. In: Blum, M.D., Marriott, S.B., Leclair, S.F. (Eds.), Fluvial Sedimentology VII: IAS (International Association of Sedimentologists) Special Publication, 35, pp. 257–275.

Amorosi, A., Milli, S., 2001. Late Quaternary depositional architecture of Po and Tevere river deltas (Italy) and worldwide comparison with coeval deltaic successions. Sedimentary Geology 144, 357–375.

Amorosi, A., Centineo, M.C., Colalongo, M.L., Pasini, G., Sarti, G., Vaiani, S.C., 2003. Facies architecture and Latest Pleistocene–Holocene depositional history of the Po Delta (Comacchio area), Italy. Journal of Geology 111, 39–56.

Amorosi, A., Colalongo, M.L., Fiorini, F., Fusco, F., Pasini, G., Vaiani, S.C., Sarti, G., 2004. Palaeogeographic and palaeoclimatic evolution of the Po Plain from 150-ky core records. Global and Planetary Change 40, 55–78.

Amorosi, A., Centineo, M.C., Colalongo, M.L., Fiorini, F., 2005. Millennial-scale depositional cycles from the Holocene of the Po Plain, Italy. Marine Geology 222–223, 7–18.

Amorosi, A., Sarti, G., Rossi, V., Fontana, V., 2008. Anatomy and sequence stratigraphy of the late Quaternary Arno valley fill (Tuscany, Italy). In: Amorosi, A., Haq, B.U., Sabato, L. (Eds.), Advances in application of sequence stratigraphy in Italy: GeoActa, Special Publication, 1, pp. 55–66.

Amorosi, A., Rossi, V., Sarti, G., Mattei, R., 2011. Coalescent valley fills from the late Quaternary record of Tuscany (Italy). Quaternary International. http://dx.doi.org/10.1016/j.quaint.2011.10.015.

Asioli, A., Trincardi, F., Correggiari, A., Langone, L., Vigliotti, L., Van Der Kaars, S., Lowe, J., 1996. The late-Quaternary deglaciation in the Central Adriatic basin. Il Quaternario, Italian Journal of Quaternary Sciences 9, 763–770.

Barber, D.C., Dyke, A., Hillaire-Marcel, C., Jennings, A.E., Andrews, J.T., Kerwin, M.W., Bilodeau, G., McNeely, R., Southon, J., Morehead, M.D., Gagnon, J.-M., 1999. Forcing of the cold event of 8,200 years ago by catastrophic drainage of Laurentide lakes. Nature 400, 344–348. http://dx.doi.org/10.1038/22504.

Barberi, F., Buanasorte, G., Cioni, R., Fiordelisi, A., Foresi, L., Iaccarino, S., Laurenzi, M.A., Sbrana, A., Vernia, L., Villa, I.M., 1994. Plio-Pleistocene geological evolution of the geothermal area of Tuscany and Lazio. Memorie descrittive della Carta Geologica d'Italia 49, 77–134.

Bard, E., Hamelin, B., Arnold, M., Montaggionis, L., Cabiochll, G., Faurell, G., Rougerie, F., 1996. Deglacial sea-level record from Tahiti corals and the timing of global meltwater discharge. Nature 382, 241–244.

Bard, E., Hamelin, B., Delanghe-Sabatier, D., 2010. Deglacial meltwater pulse 1B and Younger Dryas sea levels revisited with boreholes at Tahiti. Science 327, 1235–1237.

Barmawidjaja, D.M., Jorissen, F.J., Puskaric, S., Van der Zwaan, G.J., 1992. Microhabitat selection by benthic foraminifera in the Northern Adriatica Sea. Journal of Foraminiferal Research 22, 297–317.

Barra, D., Bonaduce, G., Brancaccio, L., Cinque, A., Ortolani, F., Pagliuca, S., Russo, F., 1992. Evoluzione olocenica della piana costiera del Fiume Sarno (Campania). Memorie della Società Geologica Italiana 42, 255–267.
Bellini, C., Mariotti Lippi, M., Montanari, C., 2009. The Holocene landscape history of the NW Italian coasts. The Holocene 19, 1161–1172.
Bellotti, P., 2000. Il modello morfosedimentario dei maggiori delta tirrenici italiani. Bollettino della Societa Geologica Italiana 119, 777–792.
Bellotti, P., Chiocchini, U., Cipriani, N., Milli, S., 1993. I sistemi deposizionali nei sedimenti clastici pleistocenici affioranti nei dintorni di Ponte Galeria (sud ovest di Roma). Bollettino della Societa Geologica Italiana 112, 923–941.
Bellotti, P., Chiocci, F.L., Milli, S., Tortora, P., Valeri, P., 1994. Sequence stratigraphy and depositional setting if the Tiber delta: integration of high-resolution seismics, well logs, and archeological data. Journal of Sedimentary Research B64, 416–432.
Bellotti, P., Milli, S., Tortora, P., Valeri, P., 1995. Physical stratigraphy and sedimentology of the late Pleistocene–Holocene Tiber Delta depositional sequence. Sedimentology 42, 617–634.
Bellotti, P., Caputo, C., Davoli, L., Evangelista, S., Garzanti, E., Pugliese, F., Valeri, P., 2004. Morpho-sedimentary characteristics and Holocene evolution of the Ombrone river Delta (Southern Tuscany). Geomorphology 61, 71–90.
Bellotti, P., Calderoni, G., Carboni, M.G., Di Bella, L., Tortora, P., Valeri, P., Zernitskaya, V., 2007. Late Quaternary landscape evolution of the Tiber River delta plain (Central Italy): new evidence from pollen data, biostratigraphy and ^{14}C dating. Zeitschrift für Geomorphologie N.E. 4, 505–534.
Bellotti, P., Mattei, M., Tortora, P., Valeri, P., 2009. Geoarchaeological investigations in the area of the imperial harbours of Rome. Méditerranée 112, 51–58.
Bellotti, P., Calderoni, G., Di Rita, F., D'Orefice, M., D'Amico, C., Esu, D., Magri, D., Preite Martinez, M., Tortora, P., Valeri, P., 2011. The Tiber river delta plain (central Italy): coastal evolution and implications for the ancient Ostia Roman settlement. The Holocene 21, 1105–1116. http://dx.doi.org/10.1177/0959683611400464.
Belluomini, G., Iuzzolini, P., Manfra, L., Mortari, R., Zalaffi, M., 1986. Evoluzione recente del delta del Tevere. Geologica Romana 25, 213–224.
Bergamin, L., Di Bella, L., Frezza, V., Devoti, S., Nisi, M.F., Silenzi, S., Carboni, M.G., 2006. Late Quaternary Palaeoenvironmental Evolution and sea-level Changes at the Versilian Coast (Tuscany, Italy): Micropalaeontological Proxies. In: Coccioni, R., Marsili, A. (Eds.), Proceedings of the Second and Third Italian Meetings of Environmental Micropaleontology: Grzybozsky Foundation Special Publication, 11, pp. 1–11.
Berné, S., Baton, J.M., Delpeint, A., Dennielou, B., Duval, F., Field, M., Lericolais, G., Le Roux, E., Satra, C., Taviani, M., 2003. Deglacial History of the Rhône Prodelta from Detailed Morphology and Preliminary Stratigraphic Data. Open Conference on Comparing Mediterranean and Black Sea prodeltas. 26–28 October 2003, Abstract Book Aix-en-Provence, France, pp. 7–8.
Bhattacharia, J.P., Giosan, L., 2003. Wave-influenced deltas: geomorphological implications for facies reconstruction. Sedimentology 50, 187–210.
Bhattacharya, J.P., 2006. Deltas. In: Posamentier, H.W., Walker, R.G. (Eds.), Facies Models Revisited: SEPM (Society for Sedimentary Geology) Special Publication, 84, pp. 237–292.
Bhattacharya, J.P., Walker, R.G., 1992. Deltas. In: Walker, R.G., James, N.P. (Eds.), Facies Models: Response to Sea Level Change. Geological Association of Canada, pp. 157–177.
Bird, M.I., Fifield, L.K., Teh, T.S., Chang, C.H., Shirlaw, N., Lambeck, K., 2007. An inflection in the rate of early mid-Holocene eustatic sea-level rise: a new sea-level curve from Singapore. Estuarine, Coastal and Shelf Sciences 71, 523–536.
Blum, M.D., Aslan, A., 2006. Signatures of climate vs. sea-level change within incised valley-fill successions: Quaternary examples from the Texas Gulf Coast. Sedimentary Geology 190, 177–211.
Blum, M.D., Price, D.M., 1998. Quaternary alluvial plain construction in response to interacting glacio-eustatic and climatic controls, Texas Gulf Costal Plain. In: Shanley, K.W., McCabe, P.J. (Eds.), Relative role of eustasy, climate, and tectonism in continental rocks: SEPM (Society for Sedimentary Geology) Special Publication, 59, pp. 31–48.
Blum, M.D., Törnqvist, T.E., 2000. Fluvial response to climate and sea-level change: a review and look forward. Sedimentology 47 (Suppl. 1), 2–48.
Bodergat, A.M., Ikeya, N., Irzi, Z., 1998. Domestic and industrial pollution: use of ostracods (Crustacea) as sentinels in the marine coastal environment. Journal de Recherches Oceanographique 23, 139–144.
Bond, G., Showers, W., Cheseby, M., Lotti, R., Almasi, P., deMenocal, P., Priore, P., Cullen, H., Hajdas, I., Bonani, G., 1997. A pervasive millennial-scale cycle in North Atlantic Holocene and glacial climates. Science 278, 1257–1266.
Bordoni, P., Valensise, G., 1998. Deformation of the 125 ka Marine Terrace in Italy: Tectonic Implications. In: Stewart, I.S., Vita-Finzi, C. (Eds.), Coastal Tectonics: Geological Society London, Special Publication, 146, pp. 71–110.
Bottema, S., 1975. The interpretation of pollen spectra from prehistoric settlements (with special attention to Liguliflorae). Palaeohistoria 17, 17–35.
Boyd, R., Dalrymple, R.W., Zaitlin, B.A., 2006. Estuarine and Incised-valley Facies Models. In: Posamentier, H.W., Walker, R.G. (Eds.), Facies Models Revisited: SEPM (Society for Sedimentary Geology) Special Publication, 84, pp. 171–235.
Boyer, J., Duvail, C., Le Strat, P., Gensous, B., Tesson, M., 2005. High resolution stratigraphy and evolution of the Rhône delta plain during postglacial time, from subsurface drilling data bank. Marine Geology 222–223, 267–298.
Cabral, M.C., Freitas, M.C., Andrade, C., Cruces, A., 2006. Coastal evolution and Holocene ostracods in Melides lagoon (SW Portugal). Marine Micropaleontology 60, 181–204.
Caputo, C., La Monica, G.B., Lupia Palmieri, E., Pugliese, F., 1987. Physiographic Characteristics and Dynamics of the Shores of Rome (Italy). In: Gardiner, V. (Ed.), Proceeding of the First International Conference on Geomorphology, Part I. Wiley, Chichester, pp. 1185–1198.
Carbonel, P., 1982. Les Ostracodes, traceurs des variations hydrologiques dans les systémes de transition eau douce-eau salée. Mémoires de la Société Géologique de France 144, 117–128.
Carboni, M.G., 1993. Contributo alla stratigrafia del Quaternario laziale. Il Quaternario 6, 27–34.
Carboni, M.G., Bergamin, L., Di Bella, L., Iamundo, F., Pugliese, N., 2002. Palaeoecological evidences from foraminifers and ostracods on Late Quaternary sea-level changes in the Ombrone river plain (central Tyrrhenian coast, Italy). Geobios 35, 40–50.
Cattaneo, A., Trincardi, F., 1999. The Late Quaternary transgressive record in the Adriatic epicontinental sea: basin widening and facies partitioning. In: Bergman, K.M., Snedden, J.W. (Eds.), Isolated Shallow Marine Sand Bodies: Sequence Stratigraphic Analysis and Sedimentologic Interpretation: SEPM Special Publication, 64, pp. 127–146.
Chiocci, F.L., 2000. Depositional Response to Quaternary Fourth-order Sea-level Fluctuations on the Latium margin (Tyrrhenian Sea, Italy). In: Hunt, D., Gawthorpe, R.L. (Eds.), Sedimentary Response to Forced Regressions: Geological Society of London, Special Publication, 172, pp. 271–289.
Chiocci, F.L., Milli, S., 1995. Construction of a chronostratigraphic diagram for a high-frequency sequence: the 20 ky B.P. to present Tiber depositional sequence. Il Quaternario 8, 339–348.
Chiocci, F.L., Ercilla, G., Torres, J., 1997. Stratal architecture of Western Mediterranean Margins as the result of the stacking of Quaternary lowstand deposits below "glacio-eustatic fluctuation base-level". Sedimentary Geology 112, 195–217.
Cimerman, F., Langer, M., 1991. Mediterranean Foraminifera. Slovenska Akademija Znanosti in Umetnosti, Academia Scientiarum Artium Slovenica, Classis IV. Historia Naturalis 30, 118.
Cioni, R., Laurenzi, M.A., Sbrana, A., Villa, I.M., 1993. $^{40}Ar/^{39}Ar$ chronostratigraphy of the initial activity in the Sabatini Volcanic Complex (Italy). Bollettino della Societa Geologica Italiana 112, 251–263.
Clarke, G.K.C., Leverington, D.W., Teller, J.T., Dyke, A.S., 2004. Paleohydraulics of the last outburst flood from glacial Lake Agasiz and the 8200 BP cold event. Quaternary Sciences Review 23, 389–407.
Coleman, J.M., Wright, L.D., 1975. Modern River Deltas: Variability of Processes and Sand Bodies. In: Broussard, M.L. (Ed.), Deltas, models for exploration. Houston Geological Society, pp. 99–149.
Coutellier, V., Stanley, D.J., 1987. Late Quaternary stratigraphy and paleogeography of the eastern Nile delta, Egypt. Marine Geology 77, 257–275.
Dalrymple, R.W., Zaitlin, B.A., Boyd, R., 1992. Estuarine facies models: conceptual basis and stratigraphic implications. Journal of Sedimentary Petrology 62, 1130–1146.
Dan, S., Walstra, D.R., Stive, M.J.F., Panin, N., 2011. Processes controlling the development of a river mouth spit. Marine Geology 280, 116–129.
De Rita, D., Funiciello, R., Corda, L., Sposato, A., Rossi, U., 1993. Volcanic Unit. In: Di Filippo, M. (Ed.), Sabatini Volcanic Complex: Consiglio Nazionale Delle Ricerche, Progetto Finalizzato " Geodinamica " Monografie Finali, 11, pp. 33–79.
De Rita, D., Milli, S., Rosa, C., Zarlenga, F., Cavinato, G.P., 1994. Catastrophic eruptions and eustatic cycles: example of Lazio volcanoes. Atti dei Convegni Lincei 112, 135–142.
De Rita, D., Faccenna, C., Funiciello, R., Rosa, C., 1995. Stratigraphy and volcano-tectonics. In: Trigila, R. (Ed.), The Volcano of the Alban Hills: Tipografia S.G.S., pp. 33–71.
De Rita, D., Fabbri, M., Mazzini, I., Paccara, P., Sposato, A., Trigari, A., 2002. Volcanoclastic sedimentation in coastal environments: the interplay between volcanism and Quaternary sea level changes (central Italy). Quaternary International 95–96, 141–154.
Di Bella, L., Bellotti, P., Frezza, V., Bergamin, L., Carboni, M.G., 2011. Benthic foraminiferal assemblages of the imperial harbor of Claudius (Rome): further paleoenvironmental and geoarcheological evidences. The Holocene 21, 1245–1259. http://dx.doi.org/10.1177/0959683611405239.
Di Rita, F., Magri, D., 2012. An overview of the Holocene vegetation history from the central Mediterranean coasts. Journal of Mediterranean Earth Science 4, 35–52. http://dx.doi.org/10.3304/JMES.2012.003.
Di Rita, F., Celant, A., Magri, D., 2010. Holocene environmental instability in the wetland north of the Tiber delta (Rome, Italy): sea–lake–man interactions. Journal of Paleolimnology 44, 51–67. http://dx.doi.org/10.1007/s10933-009-9385-9.
Di Rita, F., Anzidei, A.P., Magri, D., 2012. A Lateglacial and early Holocene pollen record from Valle di Castiglione (Rome): vegetation dynamics and climate implications. Quaternary International. http://dx.doi.org/10.1016/j.quaint.2011.11.011.
Doglioni, C., Innocenti, F., Morellato, C., Procaccianti, D., Scrocca, D., 2004. On the Tyrrhenian sea opening. Memorie descrittive della Carta Geologica d'Italia 44, 147–164.
Drescher-Schneider, R., de Beaulieu, J.-L., Magny, M., Walter-Simonnet, A.-V., Bossuet, G., Millet, L., Brugiapaglia, E., Drescher, A., 2007. Vegetation history, climate and human impact over the last 15,000 years at Lago dell'Accesa (Tuscany, Central Italy). Vegetation History and Archaeobotany 16, 279–299.
Ercilla, G., Alonso, B., Baraza, J., 1994. Post-Calabrian sequence stratigraphy of the northwestern Alboran Sea (southwestern Mediterranean). Marine Geology 120, 249–265.
Fielding, C.R., Gibling, M.R., 2005. Distinguishing Between Channel and Valley Fills: Definitions, Diagnostic Criteria and Dimensional Data. 8th International Conference on Fluvial Sedimentology, Delft, Netherlands, p. 101.
Fiorini, F., Vaiani, S.C., 2001. Benthic foraminifer and transgressive–regressive cycles in the Late Quaternary subsurface sediments of the Po Plain near Ravenna (Northern Italy). Bollettino della Società Palaeontologica Italiana 40, 357–403.
Follieri, M., Magri, D., Sadori, L., 1988. 250,000-year pollen record from Valle di Castiglione (Roma). Pollen et Spores 30, 329–356.
Frenzel, P., Boomer, I., 2005. The use of ostracods from marginal marine, brackish waters as bioindicators of modern and Quaternary environmental change. Palaeogeography, Palaeoclimatology, Palaeoecology 225, 68–92.
Frezza, V., Carboni, M.G., 2009. Distribution of recent foraminiferal assemblages near the Ombrone River mouth (Northern Tyrrhenian Sea, Italy). Revue de Micropaleontologie 52, 43–66.
Funiciello, R., Locardi, E., Parotto, M., 1976. Lineamenti geologici dell'area sabatina orientale. Bollettino della Societa Geologica Italiana 95, 831–849.

Gibling, M.R., 2006. Width and thickness of fluvial channel bodies and valley fills in the geological record: a literature compilation and classification. Journal of Sedimentary Research 76, 731–770.
Giordano, G., Esposito, A., De Rita, D., Fabbri, M., Mazzini, I., Trigari, A., Rosa, C., Funiciello, R., 2003. The sedimentation along the roman coast between middle and upper Pleistocene: the interplay of eustatism, tectonics and volcanism – new data and review. Il Quaternario 16 (1Bis), 121–129.
Giosan, L., 2007. Morphodynamic Feedbacks on Deltaic Coasts: Lessons from the Wave Dominated Danube Delta. Proceedings of Coastal Sediments 2007. ASCE, New Orleans, U.S.A., pp. 828–841.
Giosan, L., Donnelly, J., Vespremeanu, E., Bhattacharya, J., Olariu, C., Buonaiuto, F., 2005. River Delta Morphodynamics: Examples from the Danube Delta. In: Giosan, L., Bhattacharya, J.P. (Eds.), River Deltas: Concepts, Models, Examples: SEPM (Society for Sedimentary Geology), Special Publication, 83, pp. 393–411.
Giraudi, C., 2004. Evoluzione tardo-olocenica del delta del Tevere. Il Quaternario 17, 477–492.
Giraudi, C., 2011. The sediments of the 'Stagno di Maccarese' marsh (Tiber river delta, central Italy): a late-Holocene record of natural and human-induced environmental changes. The Holocene 21, 1233–1243. http://dx.doi.org/10.1177/0959683611405235.
Giraudi, C., Tata, C., Paroli, L., 2009. Late Holocene evolution of Tiber River Delta and geoarchaeology of Claudius and Trajan Harbor, Rome. Geoarchaeology 24, 371–382.
Goiran, J.P., Tronchère, H., Salomon, F., Carbonel, P., Djerbi, H., Ognard, C., 2009. Paleoenvironmental recontruction of the ancient harbors of Rome: Claudius and Trajan's marine harbors on the Tiber delta. Quaternary International 216, 3–13.
Gouw, M.J.P., Erkens, G., 2007. Architecture of the Holocene Rhine-Meuse delta (the Netherlands) – a result of changing external controls. The Holocene 86, 23–54.
Guernet, C., Lemeille, F., Sorel, D., Bourdillon, C., Berge-Thierry, C., Manakou, M., 2003. Les Ostracodes et le Quaternaire d'Aigion (golfe de Corinthe, Grèce). Revue de Micropaleontologie 46, 73–93.
Haq, B.U., Hardenbol, J., Vail, P.R., 1988. Mesozoic and Cenozoic Chronostratigraphy and Cycles of Sea-level Change. In: Wilgus, C.K., Hastings, B.S., Kendall, C.G.St.C., Posamentier, H.W., Ross, C.A., Van Wagoner, J.C. (Eds.), Sea-level changes: an integrated approach: SEPM (Society for Sedimentary Geology) Special Publication, 42, pp. 71–108.
Hardenbol, J., Thierry, J., Farley, M.B., Jacquin, T., De Graciansky, P.C., Vail, P.R., 1998. Mesozoic and Cenozoic Sequence Chronostratigraphic Framework of European Basins. In: De Graciansky, P.C., Hardenbol, J., Thierry, J., Vail, P.R. (Eds.), Mesozoic and Cenozoic Sequence Stratigraphy of European Basins: SEPM (Society for Sedimentary Geology) Special Publication, 60, pp. 3–13.
Havinga, A.J., 1984. A 20-year experimental investigation into the differential corrosion susceptibility of pollen and spores in various soil types. Pollen et Spores 26, 541–558.
Hernández-Molina, F.J., Somoza, L., Rey, J., Pomar, L., 1994. Late Pleistocene-Holocene sediments on the Spanish continental shelves: model for very high resolution sequence stratigraphy. Marine Geology 120, 129–174.
Hernández-Molina, F.J., Somoza, L., Rey, J., 1996. Late Pleistocene–Holocene High Resolution Sequence Analysis on the Alboran Sea Continental Shelf. In: De Batist, M., Jacobs, P. (Eds.), Geology of Siliciclastic Shelf Seas: Geological Society of London, Special Publication, 117, pp. 139–154.
Hernández-Molina, F.J., Fernández-Salas, L.M., Lobo, F., Somoza, L., Díaz-del-Río, V., Alveirinho Dias, J.M., 2000. The infralittoral prograding wedge: a new large-scale progradational sedimentary body in shallow marine environments. Geo-Marine Letters 20, 109–117.
Hijma, M.P., Cohen, K.M., 2010. Timing and magnitude of the sea-level jump preluding the 8200 yr event. Geology 38, 275–278.
Hori, K., Saito, Y., 2007. An early Holocene sea-level jump and delta initiaton. Geophysical Research Letters 34, L18401. http://dx.doi.org/10.1029/2007GL031029.
Incarbona, A., Di Stefano, E., Sprovieri, R., Bonomo, S., Pelosi, N., Sprovieri, M., 2010. Millennial-scale paleoenvironmental changes in the central Mediterranean during the last interglacial: comparison with European and North Atlantic records. Geobios 43, 111–122.
Jorissen, F.J., 1988. Benthic foraminifera from the Adriatic Sea; principles of phenotypic variations. Utrecht Micropalaeontological Bulletins 37, 1–174.
Karner, D.B., Marra, F., Renne, P.R., 2001. The history of the Monti Sabatini and Alban Hills volcanoes: groundwork for assessing volcanic–tectonic hazards for Rome. Journal of Volcanology and Geothermal Research 107, 185–219.
Labaune, C., Jouet, G., Berne´, S., Gensous, B., Tesson, M., Delpeint, A., 2005. Seismic stratigraphy of the deglacial deposits of the Rhône prodelta and of the adjacent shelf. Marine Geology 222–223, 299–311.
Lambeck, K., Yokoyama, Y., Purcell, T., 2002. Into and out of the Last Glacial Maximum: sea-level change during oxygen isotope stages 3 and 2. Quaternary Science Reviews 21, 343–360.
Langer, M., 1993. Epiphytic foraminifera. Marine Micropaleontology 20, 235–265.
Locardi, E., Lombardi, G., Funiciello, R., Parotto, M., 1976. The main volcanic group of Lazio (Italy): relations between structural evolution and petrogenesis. Geologica Romana 15, 279–300.
Magri, D., 1999. Late-Quaternary vegetation history at Lagaccione near Lago di Bolsena (central Italy). Review of Palaeobotany and Palynology 106, 171–208.
Malinverno, A., Ryan, W.B.F., 1986. Extension in the Tyrrhenian Sea and shortening in the Apennines as a result of arc migration driven by sinking of the lithosphere. Tectonics 5, 227–245.
Mariani, M., Prato, R., 1988. I bacini Neogenici costieri del margine tirrenico: approccio sismico-stratigrafico. Memorie della Società Geologica Italiana 41, 519–531.
Marra, F., Rosa, C., De Rita, D., Funiciello, R., 1998. Stratigraphic and tectonic features of the Middle Pleistocene sedimentary and volcanic deposits in the area of Rome (Italy). Quaternary International 47 (48), 51–63.
Martin, J., Cantelli, A., Paola, C., Blum, M., Wolinsky, M., 2011. Quantitative modeling of the evolution and geometry of incised valleys. Journal of Sedimentary Research 81, 64–79. http://dx.doi.org/10.2110/jsr.2011.5.
Martinsen, O.J., Helland Hansen, W., 1994. Sequence stratigraphy and facies models of an incised valley fill: the Gironde Estuary, France – Discussion. Journal of Sedimentary Research B64, 78–80.
Mazzini, I., Anadon, P., Barbieri, M., Castorina, F., Ferreli, L., Gliozzi, E., Mola, M., Vittori, E., 1999. Late Quaternary sea-level changes along the Tyrrhenian coast near Orbetello (Tuscany, central Italy): palaeoenvironmental reconstruction using ostracods. Marine Micropaleontology 37, 289–311.
Mendes, I., Gonzales, R., Dias, J.M.A., Lobo, F., Martins, V., 2004. Factors influencing recent benthic foraminifera distribution on the Guadiana shelf (Southwestern Iberia). Marine Micropaleontology 51, 171–192.
Milli, S., 1994. High-frequency sequence stratigraphy of the middle-late Pleistocene to Holocene deposits of the Roman Basin (Rome, Italy): relationships among high-frequency eustatic cycles, tectonics and volcanism. In: Posamentier, H.W., Mutti, E. (Eds.), Second High-Resolution Sequence Stratigraphy Conference. Tremp, Spain, 20–27 June 1994.
Milli, S., 1997. Depositional setting and high-frequency sequence stratigraphy of the middle-upper Pleistocene to Holocene deposits of the Roman basin. Geologica Romana 33, 99–136.
Milli, S., Palombo, M.R., 2011. Stratigrafia fisica e assetto deposizionale della successione del tardo Pleistocene inferiore/Olocene del Bacino Romano. In: Milli, S., Palombo, M.R., Anzidei, A.P. (Eds.), I depositi pleistocenici di Ponte Galeria e la Polledrara di Cecanibbio. Congresso Aiqua Roma, 2011 - Il Quaternario Italiano - Conoscenze e prospettive. Guida all'Escursione Post-Congresso Roma 26 Febbraio 2011, pp. 2–27.
Milli, S., Moscatelli, M., Palombo, M.R., Parlagreco, L., Paciucci, M., 2008. Incised valleys, their filling and mammal fossil record: a case study from Middle-Upper Pleistocene deposits of the Roman Basin (Latium, Italy). In: Amorosi, A., Haq, B.U., Sabato, L. (Eds.), Advances in Application of Sequence Stratigraphy in Italy: GeoActa Special Publication, 1, pp. 67–87.
Mitchum Jr., R.M., Van Wagoner, J.C., 1991. High-frequency Sequences and Their Stacking Pattern: Sequence Stratigraphy Evidence of High-frequence Eustatic Cycles. Sedimentary Geology 70, 131–170.
Montenegro, M.E., Pugliese, N., 1995. Ostracodi della laguna di Orbetello: tolleranza ed opportunismo. Atti del Museo Geologico-Paleontologico di Monfalcone, Quaderni Speciali 3, 71–80.
Montenegro, M.E., Pugliese, N., 1996. Autecological remarks on the ostracod distribution in the Marano and Grado Lagoons (Northern Adriatic Sea, Italy). In: Cherchi, A. (Ed.), Autecology of Selected Fossil Organisms: Achievements and Problems: Bollettino della Società Paleontologica Italiana, Special volume no. 3, pp. 123–132.
Montenegro, M.E., Pugliese, N., Bonaduce, G., 1998. Shelf Ostracods distribution in the Italian seas. Bulletin des Centres de Recherches Elf Exploration Production Mémoire 20, 91–101.
Neale, J.V., 1988. Ostracods and paleosalinity reconstruction. In: De Deckker, P., Colin, J.-P., Peypouquet, J.-P. (Eds.), Ostracoda in the Earth Sciences. Elsevier, Amsterdam, pp. 125–155.
Nichol, S.L., Boyd, R., Penland, S., 1994. Stratigraphic Response of Wave-dominated Estuaries to Different Relative Sea-level Changes and Sediment Supply Histories: Quaternary Case Studies from Nova Scozia, Louisiana and Eastern Australia. In: Dalrymple, R.W., Boyd, R., Zaitlin, B.A. (Eds.), Incised-valley Systems: Origin and Sedimentary Sequences: SEPM Special Publication, 51, pp. 266–283.
Oomkens, E., 1970. Depositional sequences and sand distribution in the postglacial Rhône delta complex. In: Morgan, J.P.E. (Ed.), Deltaic Sedimentation Modern and Ancient: SEPM Special Publication, 15, pp. 198–212.
Ortolani, F., Pagliuca, S., 1999. Evoluzione geologica e geomorfologica olocenica e problemi geoambientali delle pianure costiere antropizzate della Campania. Proceedings Annual Meeting Italian Sedimentology Group CNR, Giornale di Geologia 61, 73–75.
Peltier, W.R., Fairbanks, R.G., 2006. Global glacial ice volume and Last Glacial Maximum duration from an extended Barbados sea level record. Quaternary Science Reviews 25, 3322–3337.
Penland, S., Boyd, R., Suter, J.R., 1988. Transgressive depositional systems of the Mississippi delta plain: a model for barrier shoreline and shelf sand development. Journal of Sedimentary Petrology 58, 932–949.
Posamentier, H.W., Allen, G.P., 1999. Siliciclastic sequence stratigraphy — concepts and applications. SEPM, Concepts in Sedimentology and Paleontology 7, 210.
Posamentier, H.W., Vail, P.R., 1988. Eustatic Controls on Clastic Deposition II: Sequence and Systems Tract Models. In: Wilgus, C.K., Hastings, B.S., Kendall, C.G.St.C., Posamentier, H.W., Ross, C.A., Van Wagoner, J.C. (Eds.), Sea Level Changes: An Integrated Approach: SEPM (Society for Sedimentary Geology), Special Publication, 42, pp. 125–154.
Pugliese, N., Stanley, D.J., 1991. Ostracoda, depositional environments and Late Quaternary evolution of the eastern Nile Delta, Egypt. Il Quaternario 4, 275–302.
Ramsey, B., 2005. oxcal V.3.10. Research Laboratory for Archaeology, Oxford, UK.
Reading, H.G., Collinson, J.D., 1996. Clastic Coasts. In: Reading, H.G. (Ed.), Sedimentary Environments: Processes, Facies and Stratigraphy. Blackwell Science, pp. 154–231.
Rodriguez, A.B., Hamilton, M.D., Anderson, J.B., 2000. Facies and evolution of the modern Brazos Delta, Texas; wave versus flood influence. Journal of Sedimentary Research 70, 283–295.
Ruiz Muñoz, F., González-Regalado, M.L., Borrego Flores, J., Morales, J.A., 1996. Distribución y ecologia de los Foraminíferos y Ostrácodos actuales del estuario mesomareal del Río Guardiana (SO España). Geobios 29, 513–528.
Ruiz Muñoz, F., Abad, M., Bodergat, A.M., Carbonel, P., Rodríguez-Lázaro, J., Yasuhara, M., 2005. Marine and brackish-water ostracods as sentinels of anthropogenic impacts. Earth-Science Reviews 72, 89–111.

Ruiz Muñoz, F., Abad, M., Olías, M., Galán, E., González, E., Aguilá, E., Hamoumi, N., Pulido, I., Cantano, M., 2006. The present environmental scenario of the Nador Lagoon (Morocco). Environmental Research 102, 215–229.

Russo Ermolli, E., di Pasquale, G., 2002. Vegetation dynamics of south-western Italy in the last 28 kyr inferred from pollen analysis of a Tyrrhenian Sea core. Vegetation History and Archaeobotany 11, 211–219.

Savelli, C., 2002. Time-space distribution of magmatic activity in the western Mediterranean and peripheral orogens during the past 30 Ma (a stimulus to geodynamic considerations). Journal of Geodynamics 34, 99–126.

Scandone, P., 1980. Origin of the Tyrrhenian Sea and Calabrian Arc. Bollettino della Societa Geologica Italiana 98, 27–34.

Sestini, G., 1989. Nile Delta: A Review of Depositional Environments and Geological History. In: Whateley, M.K.G., Pickering, K.T. (Eds.), Deltas: Sites and Traps for Fossil Fuels: Geological Society of London Special Publication, 41, pp. 99–127.

Sgarrella, F., Moncharmont-Zei, M., 1993. Benthic Foraminifera of the Gulf of Naples (Italy): systematics and autoecology. Bollettino della Società Palaeontologica Italiana 32, 145–264.

Sheets, B.A., Paola, C., Kelberer, J.M., 2007. Creation and Preservation of Channel-form Sand Bodies in an Experimental Alluvial System. In: Nichols, G.J., Williams, E., Paola, C. (Eds.), Sedimentary Processes, Environments and Basins—Tribute to Peter Friend: IAS Special Publication, 38, pp. 555–657.

Somoza, L., Barnolas, A., Arasa, A., Maestro, A., Rees, J.G., Hernandez-Molina, F.J., 1998. Architectural stacking pattern of the Ebro delta controller by Holocen high-frequency eustatic fluctuation, delta-lobe switching and subsidence processes. Sedimentary Geology 117, 11–32.

Stanley, D.J., Warne, A.G., 1994. Worldwide initiation of Holocene marine deltas by deceleration of sea level rise. Science 265, 228–231.

Strong, N., Paola, C., 2008. Valleys that never were: time surfaces versus stratigraphic surfaces. Journal of Sedimentary Research 78, 579–593.

Swift, D.J.P., 1975. Barrier island genesis: evidence from the central Atlantic shelf, eastern USA. Sedimentary Geology 14, 1–43.

Swift, D.J.P., Kofoed, J.W., Saulsbury, F.B., Sears, P.C., 1972. Holocene Evolution of the Shelf Surface, Central and Southern Atlantic shelf of North America. In: Swift, D.J.P., Duane, D.B., Pilkey, O.H. (Eds.), Shelf sediment transport: process and pattern. Dowden Hutchinson & Ross, Stroundsburg, PA, pp. 499–574 (Stroudsburg, Pennsylvania).

Tamura, T., Saito, Y., Sieng, S., Ben, B., Kong, M., Sim, I., Choup, S., Akiba, F., 2009. Initiation of the Mekong River delta at 8 ka: evidence from the sedimentary succession in the Cambodian lowland. Quaternary Science Reviews 28, 327–344.

Trincardi, F., Asioli, A., Cattaneo, A., Correggiari, A., Vigliotti, L., Accorsi, C.A., 1996. Transgressive offshore deposits on the Central Adriatic shelf: architecture complexity and the record of the Younger Dryas short-term event. Il Quaternario 9, 753–762.

Van Asselen, S., 2011. The contribution of peat compaction to total basin subsidence: implications for the provision of accommodation space in organic-rich deltas. Basin Research 23, 239–255. http://dx.doi.org/10.1111/j.1365-2117.2010.00482.x.

Van der Zwaan, G.J., Jorissen, F.J., 1991. Biofacial Patterns in River-induced Shell Anoxia. In: Tyson, R.V., Pearson, T.H. (Eds.), Modern and Ancient Continental Shelf Anoxia: Geological Society London, Special Publication, 58, pp. 65–82.

Van Maren, D.S., 2005. Barrier formation on an actively prograding delta system: The Red River Delta, Vietnam. Marine Geology 224, 123–143.

Wehr, F.L., 1993. Effects of variations in subsidence and sediment supply on parasequence stacking patterns. In: Weimer, P., Posamantier, H.W. (Eds.), Siliciclastic Sequence Stratigraphy: Recent Developments and Applications: AAPG Memoir, 58, pp. 369–379.

Zaitlin, B.A., Dalrymple, R.W., Boyd, R., 1994. The stratigraphic organization of incised-valley systems associated with relative sea-level change. In: Dalrymple, R.W., Boyd, R., Zaitlin, B.A. (Eds.), Incised-valley systems: Origin and sedimentary sequences: SEPM Special Publication, 51, pp. 45–60.